

Joint Design of Transmit Waveform and Receive Filter for MIMO Radar with One-Bit DACs/ADCs

Minglong Deng, Ziyang Cheng, *IEEE Member*, and Zishu He

Abstract—Adopting extremely low-resolution (e.g. one-bit) analog-to-digital converters (ADCs) and digital-to-analog converters (DACs) is able to bring a remarkable saving of low-cost and circuit power for multiple-input multiple-output (MIMO) radar. In this paper, the problem of joint design of transmit waveform and receive filter for collocated MIMO radar with a architecture of one-bit ADCs and DACs is investigated. Under this architecture, we derive the output quantized signal-to-interference-plus-noise ratio (QSINR), which is relative to the detection performance of target, in the presence of signal-dependent interference. The optimization problem is formulated by maximizing the QSINR with a binary waveform constraint. Due to the nonconvex objective and binary constraint, the resulting problem is hard to be directly solved. To this end, we propose an alternating minimization algorithm. More concretely, at each iteration, the closed-form solution of the receive filter is attained by exploiting the minimum variance distortionless response (MVDR) method, and then the one-bit waveform is optimized with the aid of the alternating direction method of multipliers (ADMM) algorithm. In addition, the performance gap between the one-bit MIMO radar and infinite-bit MIMO radar is theoretically analyzed under the noise-only case. Several numerical simulations are provided to demonstrate the effectiveness of the proposed methods.

Index Terms—Multiple-input and multiple-output (MIMO) radar, one-bit ADCs/DACs, quantized signal-to-interference-plus-noise ratio (QSINR), alternating direction method of multipliers (ADMM), waveform design.

I. INTRODUCTION

DURING the past few years, multiple-input and multiple-output (MIMO) radar, as an enhanced version of traditional phased-array radar, has received great attention due to its more flexible transmit scheme [1]–[9]. Compared with the phased-array radar which emits a single waveform, the MIMO radar transmits multiple waveforms that may be correlated or uncorrelated with each other. Such waveform diversity provides MIMO radar with many performance improvements, such as enhanced parameter identifiability [2], higher direction-of-arrival (DOA) estimation accuracy [3], [4], better transmitting behaviors [5]–[7], as well as improved ability of interference suppressing [8], [9].

Waveform design is one of the most effective ways to achieve above mentioned performance improvements. Many performance metrics have been taken into account to design the MIMO radar waveforms, such as the Cramer Rao bound (CRB) [10], [11], mutual information (MI) [12]–[14], and mean square error (MSE) [5]–[7], [15]–[17], to name just a few. Particularly, to improve the performance of target

detection and parameter estimation for MIMO radar, the output signal-to-interference-plus-noise ratio (SINR) maximization is often raised as a figure of merit to design the waveform [8], [9], [18]–[20]. For example, in the presence of signal-independent interference, the detection probability maximization is considered to design the optimum code matrix in [8]. In the presence of signal-dependent interference, [9] proposes a gradient based algorithm to jointly design the transmit waveform and receive filter by maximizing the SINR with a priori knowledge of the target and clutter statistics. In addition, [19] proposes two sequential optimization algorithms (SOA) based on the semidefinite relaxation (SDR) method to jointly design the transmit waveform and receive filter by maximizing the SINR while keeping the constant modulus (CM) constraint as well as a similarity constraint. In order to further increase the SINR, [20] further relaxes the CM constraint to a general peak-to-average-power ratio (PAPR) constraint, and devises the block successive upper-bound minimization method of multipliers framework [21] to solve the resultant problem.

Although the theoretical research of MIMO radar has been studied very thoroughly, the practical implementation of MIMO radar still faces great challenges. For instance, all the above-mentioned methods design the waveform and receive filter by assuming ideal analog-to-digital converters (ADCs) adopted and digital-to-analog converters (DACs). However, the high-resolution ADCs and DACs will remarkably increase the circuit power consumption and high hardware-cost, especially for MIMO radar with large-scaled array. To overcome such difficulties, sub-Nyquist technology, which reduces the sampling rate of time, frequency, as well as space, is one potential method [22]–[25]. For instance, in [22], based on the compressive sampling (CS) technology [26], the angle and doppler information on potential targets from temporally and spatially under-sampled observations are obtained. In [23], a sparse array design framework is proposed for MIMO radar allowing for a remarkable reduction in the number of antennas, while still attaining performance comparable to that of a fully-digital array. Nevertheless, all existing sub-Nyquist technologies assume infinite precision sampling, and the effect of finite-bit quantization has not yet been well addressed.

In addition to the sub-Nyquist technology, the utilization of low-resolution ADCs/DACs is an efficient way to reduce the hardware complexity and power consumption. Particularly, an extreme utilization of the low-resolution ADCs/DACs is using one-bit ADCs/DACs, which has been extensively studied in communication and radar systems [27]–[38]. Specifically, for radar system with one-bit quantizations, one-bit likelihood ratio test (LRT) detector is derived and the detection performance is evaluated in [34]. To get the angle and velocity of target, [35] proposes a maximum likelihood (ML)

The authors are with the School of Information and Communication Engineering, University of Electronic Science and Technology of China (UESTC), Chengdu 611731, China (e-mail: dengminglong@126.com; zycheng@uestc.edu.cn; zshe@uestc.edu.cn).

method to recover the virtual array data matrix from one-bit observations, and then estimates the angle and doppler parameters by using the resulting data. As for the deployment of MIMO radar with one-bit DACs, in [37], an alternating optimization framework based on fast Fourier transform (FFT) is proposed to optimize the one-bit transmit signal for the large-scale MIMO systems by minimize the MSE between the designed pattern and a desired one. More recently, in [38], the one-bit transmit sequences are designed to ensure the DOA estimation accuracy of a dual-function radar-communication (DFRC) system equipped with one-bit DACs.

Note that, the above-mentioned one-bit MIMO radars do not consider the interference suppression. The existing works on the interference suppression MIMO radar, such as [9], [19], [20], assume infinite-bit ADCs and DACs are adopted at receiver and transmitter. To the best of our knowledge, the problems of the waveform design and corresponding theoretical analysis in the presence of interference for MIMO radar with one-bit DACs and ADCs have not been addressed. These motivate us to carry out this work. Specifically, the main contributions and novelties of this paper are summarized as follows:

- In the presence of signal-dependent interferences, based on the full or partial knowledges of the interferences, the expression of the output quantized SINR (QSINR) under the low input SNR case for MIMO radar with one-bit ADCs and DACs is derived in detail, and the problem of the joint design of one-bit waveform and receive filter is formulated by maximizing the one-bit QSINR.
- In order to tackle the resultant problem with a non-convex fractional quadratic objective and discrete one-bit constraint, an alternating minimization method based on the ADMM framework is devised. Particularly, in the ADMM framework, the closed-form solution of each primal variable is provided. Moreover, the Karush-Kuhn-Tucher (KKT) condition of the resultant problem is analyzed under the ADMM framework.
- In noise-only scenario, the performance loss of the output QSINR caused by using one-bit ADCs and DACs is theoretically analyzed relative to the traditional infinite-bit MIMO radar.
- Several simulation experiments are presented to illustrate the effectiveness of the proposed alternating minimization algorithm in terms of the output QSINR, convergence performance, and robustness to uncertainty of interference.

The rest of this paper is organized as follows. In Section II, we give the signal model and formulate the optimization problem. In Section III, we show how to solve the optimization problem. Finally, simulation results and conclusions are given in Section V and VI, respectively.

Notations: For conciseness of introducing the ensuing contents, the italic letter a (or A), boldface letter \mathbf{a} , and upper case boldface letter \mathbf{A} are denoted as a scalar, a vector, and a matrix, respectively. The transpose and conjugate transpose operators are given by $(\cdot)^T$ and $(\cdot)^H$, respectively. $\|\cdot\|_1$ and $\|\cdot\|_2$ denote the l_1 and l_2 norm of a vector, respectively. Script letters \mathcal{U} , \mathcal{N} , and \mathcal{CN} are used for denoting uniform,

Gaussian, and complex Gaussian distributions. The operators $\text{vec}(\cdot)$, \odot , \otimes , and $\mathbb{E}\{\cdot\}$ represent the vectorization operation, element product, Kronecker product, and statistical expectation, respectively. The $\Re\{\cdot\}$ and $\Im\{\cdot\}$ are employed to get the real and imaginary part of a complex variable. The sets of real and complex numbers are denoted by \mathbb{R} and \mathbb{C} .

II. PRELIMINARIES

A. Signal Model

We consider a collocated MIMO radar system which is equipped with N_t transmit and N_r receive antennas. The transmit and receive arrays are assumed to be half-wavelength spaced uniform linear arrays (ULAs). Let $s_n(l)$ be the l th ($l = 1, 2, \dots, L$) sample of the transmit signal of the n th ($n = 1, 2, \dots, N_t$) antenna, where L is the total number of samples within a pulse width. Suppose that there exists K signal-dependent interferences (e.g., clutters), the receive signal at the receive array can be expressed as [19]

$$\mathbf{x}(l) = \xi_0 \mathbf{a}_r(\theta_0) \mathbf{a}_t^T(\theta_0) \mathbf{s}(l) + \sum_{k=1}^K \xi_k \mathbf{a}_r(\theta_k) \mathbf{a}_t^T(\theta_k) \mathbf{s}(l) + \mathbf{v}(l) \quad (1)$$

where θ_0 and ξ_0 denote the direction and complex reflection coefficient of the target of interest, θ_k and ξ_k ($k = 1, 2, \dots, K$) are the directions and complex amplitudes of the k -th interference, $\mathbf{s}(l) = [s_1(l), s_2(l), \dots, s_{N_t}(l)]^T$ is the transmit signal vector, $\mathbf{v}(l) \in \mathbb{C}^{N_r \times 1}$ denotes the noise vector, which is assumed to obey the complex Gaussian distribution with zero mean and covariance matrix $\sigma^2 \mathbf{I}_{N_r}$. $\mathbf{a}_r(\theta)$ and $\mathbf{a}_t(\theta)$ are the receive and transmit steering vectors, defined as

$$\mathbf{a}_r(\theta) = \frac{1}{\sqrt{N_r}} [1, e^{-j\pi \sin \theta}, \dots, e^{-j\pi(N_r-1) \sin \theta}]^T \quad (2a)$$

$$\mathbf{a}_t(\theta) = \frac{1}{\sqrt{N_t}} [1, e^{-j\pi \sin \theta}, \dots, e^{-j\pi(N_t-1) \sin \theta}]^T \quad (2b)$$

Collecting all L discrete samples into a tall vector $\mathbf{x} \in \mathbb{C}^{N_r L \times 1}$ yields

$$\mathbf{x} = \xi_0 \mathbf{A}(\theta_0) \mathbf{s} + \sum_{k=1}^K \xi_k \mathbf{A}(\theta_k) \mathbf{s} + \mathbf{v} \quad (3)$$

where $\mathbf{x} = [\mathbf{x}^T(1), \dots, \mathbf{x}^T(L)]^T$, $\mathbf{s} = [\mathbf{s}^T(1), \dots, \mathbf{s}^T(L)]^T$, $\mathbf{v} = [\mathbf{v}^T(1), \dots, \mathbf{v}^T(L)]^T$, and $\mathbf{A}(\theta) = \mathbf{I}_L \otimes \mathbf{a}_r(\theta) \mathbf{a}_t^T(\theta)$.

In order to reduce hardware cost remarkably, in our considered model, we assume that the transmit and receive arrays are equipped with one-bit DACs and one-bit ADCs. Specifically, each antenna is configured with two one-bit quantizers to quantize the real and imaginary parts of a complex signal. For the transmit end, with assumption of unit energy, the transmit alphabet \mathcal{X} is $\frac{1}{\sqrt{2N_t L}} \{1 + j, 1 - j, -1 + j, -1 - j\}$ [37], [38]. While for the receive array, the quantized output of the baseband receive signal is expressed as

$$\mathbf{y} = \mathcal{Q}(\mathbf{x}) \quad (4)$$

where $\mathcal{Q}(x) = \text{sign}(\Re\{x\}) + j \text{sign}(\Im\{x\})$ denotes the complex-valued one-bit quantization function.

B. Quantized SINR

Define receive filter $\mathbf{w} \in \mathbb{C}^{N_r L \times 1}$, the output signal can be given by $z = \mathbf{w}^H \mathbf{y}$. Since the goal of designing receive filter is to distinguish whether the target exists, we take the ratio of average output power in the presence of target to that in the absence of target, i.e., the quantized signal-to-interference-plus-noise ratio (QSINR), as the optimization metric, defined as

$$\begin{aligned} \text{QSINR} &= \frac{\mathbb{E} \left\{ \left| \mathbf{w}^H \mathcal{Q} \left(\xi_0 \mathbf{A}(\theta_0) \mathbf{s} + \sum_{k=1}^K \xi_k \mathbf{A}(\theta_k) \mathbf{s} + \mathbf{v} \right) \right|^2 \right\}}{\mathbb{E} \left\{ \left| \mathbf{w}^H \mathcal{Q} \left(\sum_{k=1}^K \xi_k \mathbf{A}(\theta_k) \mathbf{s} + \mathbf{v} \right) \right|^2 \right\}} \\ &= \frac{\mathbf{w}^H \mathbf{R}_1 \mathbf{w}}{\mathbf{w}^H \mathbf{R}_0 \mathbf{w}} \end{aligned} \quad (5)$$

where \mathbf{R}_1 and \mathbf{R}_0 are given by

$$\mathbf{R}_1 = \mathbb{E} \left\{ \mathcal{Q}(\mathbf{h}_1 + \mathbf{v}) \mathcal{Q}(\mathbf{h}_1 + \mathbf{v})^H \right\} \quad (6a)$$

$$\mathbf{R}_0 = \mathbb{E} \left\{ \mathcal{Q}(\mathbf{h}_0 + \mathbf{v}) \mathcal{Q}(\mathbf{h}_0 + \mathbf{v})^H \right\} \quad (6b)$$

with $\mathbf{h}_1 = \xi_0 \mathbf{A}(\theta_0) \mathbf{s} + \sum_{k=1}^K \xi_k \mathbf{A}(\theta_k) \mathbf{s}$ and $\mathbf{h}_0 = \sum_{k=1}^K \xi_k \mathbf{A}(\theta_k) \mathbf{s}$.

To compute the matrices \mathbf{R}_1 and \mathbf{R}_0 , the following Proposition is useful.

Proposition 1: For two complex numbers $x_1 = \tau_1 + v_1$ and $x_2 = \tau_2 + v_2$, where τ_1 and τ_2 are complex constants, and v_1 and v_2 are two independent and identically distributed (IID) complex Gaussian variables with distributions of $\mathcal{CN}(0, \sigma^2)$, let us denote $y_1 = \mathcal{Q}(x_1)$ and $y_2 = \mathcal{Q}(x_2)$, then the correlation of y_1 and y_2 can be expressed as

$$\begin{aligned} \mathbb{E} \{ y_1 y_2^* \} &= \left[\text{erf} \left(\frac{\Re \{ \tau_1 \}}{\sigma} \right) + j \text{erf} \left(\frac{\Im \{ \tau_1 \}}{\sigma} \right) \right] \\ &\quad \times \left[\text{erf} \left(\frac{\Re \{ \tau_2 \}}{\sigma} \right) - j \text{erf} \left(\frac{\Im \{ \tau_2 \}}{\sigma} \right) \right] \end{aligned} \quad (7)$$

where the function $\text{erf}(x) = \frac{2}{\sqrt{\pi}} \int_0^x e^{-t^2} dt$.

Proof: see **Appendix A**. ■

To simplify (7), we provide the following Lemma.

Lemma 1: If $|\tau_1|, |\tau_2| \ll \sigma$, (7) can be further recast as

$$\mathbb{E} \{ y_1 y_2^* \} \approx \left(\frac{2}{\sqrt{\pi} \sigma} \right)^2 \tau_1 \tau_2^*. \quad (8)$$

Proof: see **Appendix B**. ■

For most radar applications, the input SNR per sample is very weak before the receive processing, which means the echo powers of the target and signal-dependent interferences are much weaker compared to the noise signal, and thus the condition $|h_{1,l}|, |h_{0,l}| \ll \sigma$ is satisfied, where $h_{1,l}$ and $h_{0,l}$ are the l th elements of \mathbf{h}_1 and \mathbf{h}_0 , respectively. As shown in Fig. 1, the estimated (obtained by 10^8 tests), approximated (using (8)), and true (using (7)) $\mathbb{E} \{ y_1 y_2^* \}$ versus the SNR ($|\tau_1|^2/\sigma^2$ or $|\tau_2|^2/\sigma^2$) are plotted. As expected, when $|\tau_1|^2/\sigma^2$ ($|\tau_2|^2/\sigma^2$) is lower than 0dB, both the amplitude and phase of the approximated $\mathbb{E} \{ y_1 y_2^* \}$ are close to that of the estimated and true $\mathbb{E} \{ y_1 y_2^* \}$.

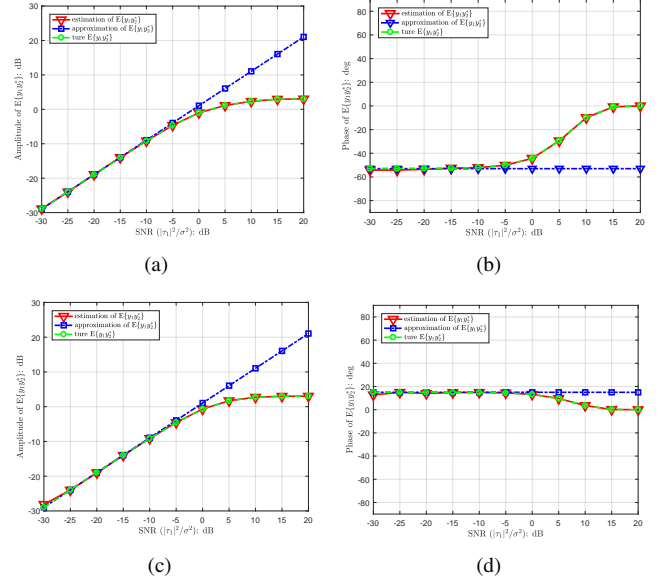


Fig. 1. The amplitude and phase of the estimated (obtained by 10^8 tests), approximated (using (8)), and true (using (7)) $\mathbb{E} \{ y_1 y_2^* \}$ versus the SNR ($|\tau_1|^2/\sigma^2$ or $|\tau_2|^2/\sigma^2$). (a)-(b) $|\tau_1| = |\tau_2|$, and the phases of τ_1 and τ_2 are 20° and 73° ; (c)-(d) $|\tau_1| = |\tau_2|$, and the phases of τ_1 and τ_2 are 70° and 55° .

With the assumption of low SNR of a single sample (i.e., $|h_{1,l}|, |h_{0,l}| \ll \sigma$) and **Lemma 1**, we obtain the expressions of \mathbf{R}_1 and \mathbf{R}_0 as

$$\mathbf{R}_i(m, n) = \begin{cases} 2, & m = n \\ \frac{4}{\pi \sigma^2} h_{i,m} h_{i,n}^*, & m \neq n \end{cases}, \quad i = 0, 1 \quad (9)$$

where $\mathbf{R}_i(m, n)$ denotes the (m, n) -th element of the matrix \mathbf{R}_i . Moreover, according to (9), \mathbf{R}_1 and \mathbf{R}_0 can further be rewritten as

$$\mathbf{R}_1 = \frac{4}{\pi \sigma^2} \mathbf{h}_1 \mathbf{h}_1^H + \sum_{l=1}^{N_r L} \left(2 - \frac{4}{\pi \sigma^2} |h_{1,l}|^2 \right) \mathbf{e}_l \mathbf{e}_l^H \quad (10a)$$

$$\mathbf{R}_0 = \frac{4}{\pi \sigma^2} \mathbf{h}_0 \mathbf{h}_0^H + \sum_{l=1}^{N_r L} \left(2 - \frac{4}{\pi \sigma^2} |h_{0,l}|^2 \right) \mathbf{e}_l \mathbf{e}_l^H \quad (10b)$$

where \mathbf{e}_l is an $N_r L \times 1$ dimensional vector, whose l th element is 1, and 0 otherwise.

Substituting (10) into (5) yields

$$\frac{\mathbf{w}^H \mathbf{R}_1 \mathbf{w}}{\mathbf{w}^H \mathbf{R}_0 \mathbf{w}} = \frac{\frac{4}{\pi \sigma^2} \mathbf{w}^H \mathbf{h}_1 \mathbf{h}_1^H \mathbf{w} + \sum_{l=1}^{N_r L} \left(2 - \frac{4}{\pi \sigma^2} |h_{1,l}|^2 \right) |w_l|^2}{\frac{4}{\pi \sigma^2} \mathbf{w}^H \mathbf{h}_0 \mathbf{h}_0^H \mathbf{w} + \sum_{l=1}^{N_r L} \left(2 - \frac{4}{\pi \sigma^2} |h_{0,l}|^2 \right) |w_l|^2} \quad (11)$$

Recalling the assumption that $|h_{1,l}|, |h_{0,l}| \ll \sigma$, yields

$$\sum_{l=1}^{N_r L} \left(2 - \frac{4}{\pi \sigma^2} |h_{i,l}|^2 \right) |w_l|^2 \approx 2 \mathbf{w}^H \mathbf{w}, \quad i = 0 \text{ or } 1 \quad (12)$$

Note that the complex reflection coefficients of the target and interferences, i.e., $\xi_0, \xi_1, \dots, \xi_K$, are usually unknown. Herein, we assume their statistical characteristics are known. Specifically, we assume $\xi_0, \xi_1, \dots, \xi_K$ are independent zero

mean random variables with variances σ_0^2 and $\sigma_k^2, k = 1, \dots, K$ [19], [20]. Then, we use the expectations $\mathbb{E}\{\mathbf{h}_1 \mathbf{h}_1^H\}$ and $\mathbb{E}\{\mathbf{h}_0 \mathbf{h}_0^H\}$ to replace $\mathbf{h}_1 \mathbf{h}_1^H$ and $\mathbf{h}_0 \mathbf{h}_0^H$ in (11), and therefore

$$\begin{aligned} \frac{\mathbf{w}^H \mathbf{R}_1 \mathbf{w}}{\mathbf{w}^H \mathbf{R}_0 \mathbf{w}} &\approx \frac{\frac{4}{\pi \sigma^2} \mathbf{w}^H \mathbb{E}\{\mathbf{h}_1 \mathbf{h}_1^H\} \mathbf{w} + 2 \mathbf{w}^H \mathbf{w}}{\frac{4}{\pi \sigma^2} \mathbf{w}^H \mathbb{E}\{\mathbf{h}_0 \mathbf{h}_0^H\} \mathbf{w} + 2 \mathbf{w}^H \mathbf{w}} \\ &= \frac{2 \text{SNR} |\mathbf{w}^H \mathbf{A}(\theta_0) \mathbf{s}|^2}{\pi \mathbf{w}^H \mathbf{\Xi}(\mathbf{s}) \mathbf{w} + \mathbf{w}^H \mathbf{w}} + 1 \\ &= \frac{2 \text{SNR} |\mathbf{w}^H \mathbf{A}(\theta_0) \mathbf{s}|^2}{\pi \mathbf{s}^H \mathbf{\Phi}(\mathbf{w}) \mathbf{s}} + 1 \end{aligned} \quad (13)$$

where $\text{SNR} = \sigma_0^2 / \sigma^2$, $\text{INR}_k = \sigma_k^2 / \sigma^2, k = 1, 2, \dots, K$, and the matrices $\mathbf{\Xi}(\mathbf{s})$ and $\mathbf{\Phi}(\mathbf{w})$ are defined as

$$\mathbf{\Xi}(\mathbf{s}) = \frac{2}{\pi} \sum_{k=1}^K \text{INR}_k \mathbf{A}(\theta_k) \mathbf{s} \mathbf{s}^H \mathbf{A}^H(\theta_k) \quad (14a)$$

$$\mathbf{\Phi}(\mathbf{w}) = \frac{2}{\pi} \sum_{k=1}^K \text{INR}_k \mathbf{A}^H(\theta_k) \mathbf{w} \mathbf{w}^H \mathbf{A}(\theta_k) + \|\mathbf{w}\|_2^2 \mathbf{I}_{N_t L} \quad (14b)$$

Remark 1: Note that, the SNR (INR) mentioned above is not the input SNR (INR) for a single observation. Here, the SNR for a single observation, i.e., the SNR per sample, is about $1/N_r L$ of that defined in (13), which is defined as

$$\text{SNR}_{\text{per}} = \frac{\text{SNR}}{N_r L} \quad (15)$$

Remark 2: From (13) and omitting the constant term, it is interesting to note that the loss of the output QSINR caused by introducing the one-bit ADCs is about $2/\pi$ relative to the MIMO system with ideal ADCs.

C. QSINR Under Stochastic Case

The objective in (13) requires full knowledge of the directions of the interferences $\theta_1, \theta_2, \dots, \theta_K$. Nevertheless, in practical applications, the exact locations of the interferences might be unknown [20]. For such scenarios, it is reasonable to assume that $\theta_1, \theta_2, \dots, \theta_K$ are independent random variables. Specifically, we consider the normalized angle $\omega = \sin \theta \in [0, 1]$ instead of θ . We assume the normalized angles of the interferences ω_k ($k = 1, 2, \dots, K$) obey uniform distribution with known means ϖ_k and uncertainty bounds δ_k , i.e.,

$$\omega_k \sim \mathcal{U}(\varpi_k - \delta_k, \varpi_k + \delta_k), \quad k = 1, 2, \dots, K \quad (16)$$

Let $\mathbf{W} \in \mathbb{C}^{N_r \times L}$ and $\mathbf{S} \in \mathbb{C}^{N_t \times 1}$ be the matrix form of \mathbf{w} and \mathbf{s} , respectively. For the case of uncertainties on the interference angles, the matrices $\mathbf{\Xi}(\mathbf{s})$ and $\mathbf{\Phi}(\mathbf{w})$ (14) can be written as

$$\mathbf{\Xi}(\mathbf{s}) = \frac{2}{\pi} \sum_{k=1}^K \text{INR}_k (\mathbf{S}^T \otimes \mathbf{I}_{N_r}) \mathbf{C}(\omega_k) (\mathbf{S}^T \otimes \mathbf{I}_{N_r})^H \quad (17a)$$

$$\begin{aligned} \mathbf{\Phi}(\mathbf{w}) &= \frac{2}{\pi} \sum_{k=1}^K \text{INR}_k (\mathbf{W}^T \otimes \mathbf{I}_{N_t}) \mathbf{D}(\omega_k) (\mathbf{W}^T \otimes \mathbf{I}_{N_t})^H \\ &\quad + \|\mathbf{w}\|_2^2 \mathbf{I}_{N_t L} \end{aligned} \quad (17b)$$

where the definitions of $\mathbf{C}(\omega_k), \mathbf{D}(\omega_k) \in \mathbb{C}^{N_t N_t \times N_r N_r}$ are given in **Appendix C**.

D. Problem Formulation

With the optimization criterion of the QSINR maximization, the problem of joint design of the transmit waveform and receive filter for MIMO radar with one-bit ADCs and DACs can be formulated as

$$\begin{aligned} \max_{\mathbf{w}, \mathbf{s}} \quad & \frac{|\mathbf{w}^H \mathbf{A}(\theta_0) \mathbf{s}|^2}{\mathbf{w}^H \mathbf{\Xi}(\mathbf{s}) \mathbf{w} + \mathbf{w}^H \mathbf{w}} \\ \text{s.t.} \quad & \mathbf{s} \in \mathcal{X}^{N_t L} \end{aligned} \quad (18)$$

It is noted that the binary constraint and the couple of \mathbf{w} and \mathbf{s} in the objective are the main difficulties in solving the problem (18). Based on the alternating optimization (AltOpt) framework, although the semidefinite relaxation (SDR) [19], [39] and block coordinate descent (BCD) [40] methods are the possible manners to deal with such problem. Nevertheless, as shall be shown later in our simulations, the two methods cannot always ensure satisfactory performance. Moreover, they may suffer from prohibitive computational burdens, especially in large $N_t L$ case. To this end, a more efficient algorithm based on the ADMM method is developed to tackle the problem.

III. SOLUTION TO THE PROBLEM (18)

In this section, we shall present the AltOpt framework to solve the problem (18). More specifically, we first optimize the receive filter \mathbf{w} with a fixed waveform \mathbf{s} , and then we use the ADMM method, which is able to converge to a KKT point, to optimize \mathbf{s} with a given \mathbf{w} .

A. Optimizing the receive filter \mathbf{w} with fixed \mathbf{s}

Firstly, for a fixed \mathbf{s} , the problem (18) w.r.t. \mathbf{w} is equivalent to

$$\max_{\mathbf{w}} \frac{|\mathbf{w}^H \mathbf{A}(\theta_0) \mathbf{s}|^2}{\mathbf{w}^H \mathbf{\Xi}(\mathbf{s}) \mathbf{w} + \mathbf{w}^H \mathbf{w}} \quad (19)$$

It is easy to know that the problem (19) is equivalent to the well-known MVDR problem, whose closed-form solution is given by

$$\mathbf{w} = \frac{(\mathbf{\Xi}(\mathbf{s}) + \mathbf{I})^{-1} \mathbf{A}(\theta_0) \mathbf{s}}{\mathbf{s}^H \mathbf{A}^H(\theta_0) (\mathbf{\Xi}(\mathbf{s}) + \mathbf{I})^{-1} \mathbf{A}(\theta_0) \mathbf{s}} \quad (20)$$

B. Optimizing the transmit waveform \mathbf{s} with fixed \mathbf{w}

For a given \mathbf{w} , the problem (18) is equivalent to

$$\min_{\mathbf{s}} \frac{\mathbf{s}^H \mathbf{\Phi}(\mathbf{w}) \mathbf{s}}{\mathbf{s}^H \mathbf{\Gamma}(\mathbf{w}) \mathbf{s}} \quad (21a)$$

$$\text{s.t.} \quad \mathbf{s} \in \mathcal{X}^{N_t L} \quad (21b)$$

where $\mathbf{\Gamma}(\mathbf{w}) = \mathbf{A}^H(\theta_0) \mathbf{w} \mathbf{w}^H \mathbf{A}(\theta_0)$.

Let

$$\tilde{\mathbf{s}} = \begin{bmatrix} \Re\{\mathbf{s}\} \\ \Im\{\mathbf{s}\} \end{bmatrix} \quad (22a)$$

$$\tilde{\mathbf{\Gamma}}(\mathbf{w}) = \begin{bmatrix} \Re\{\mathbf{\Gamma}(\mathbf{w})\} & -\Im\{\mathbf{\Gamma}(\mathbf{w})\} \\ \Im\{\mathbf{\Gamma}(\mathbf{w})\} & \Re\{\mathbf{\Gamma}(\mathbf{w})\} \end{bmatrix} \quad (22b)$$

$$\tilde{\mathbf{\Phi}}(\mathbf{w}) = \begin{bmatrix} \Re\{\mathbf{\Phi}(\mathbf{w})\} & -\Im\{\mathbf{\Phi}(\mathbf{w})\} \\ \Im\{\mathbf{\Phi}(\mathbf{w})\} & \Re\{\mathbf{\Phi}(\mathbf{w})\} \end{bmatrix} \quad (22c)$$

then we can rewrite the subproblem (21) in a real-valued form as

$$\min_{\tilde{\mathbf{s}}} \frac{\tilde{\mathbf{s}}^T \tilde{\Phi}(\mathbf{w}) \tilde{\mathbf{s}}}{\tilde{\mathbf{s}}^T \tilde{\Gamma}(\mathbf{w}) \tilde{\mathbf{s}}} \quad (23a)$$

$$\text{s.t. } \tilde{\mathbf{s}} \in \frac{1}{\sqrt{2N_t L}} \{1, -1\}^{2N_t L} \quad (23b)$$

We note that the problem (23) is a binary optimization problem with fractional quadratical objective. To make the problem easy to solve, we equivalently transform the binary constraint into the following constraints:

$$\tilde{\mathbf{s}}^T \tilde{\mathbf{s}} = 1, \quad -\frac{1}{\sqrt{2N_t L}} \mathbf{1} \leq \tilde{\mathbf{s}} \leq \frac{1}{\sqrt{2N_t L}} \mathbf{1} \quad (24)$$

Now, we apply the ADMM framework [21], [34] to solve the problem (23). Specifically, we introduce two variables $\mathbf{t}, \mathbf{r} \in \mathbb{R}^{2N_t L \times 1}$ to rewrite the problem (23) as

$$\min_{\tilde{\mathbf{s}}, \mathbf{t}, \mathbf{r}} \frac{\mathbf{t}^T \tilde{\Phi}(\mathbf{w}) \mathbf{t}}{\mathbf{r}^T \tilde{\Gamma}(\mathbf{w}) \mathbf{r}} \quad (25a)$$

$$\text{s.t. } \mathbf{t} = \tilde{\mathbf{s}}, \quad \mathbf{t}^T \mathbf{t} = 1 \quad (25b)$$

$$\mathbf{r} = \tilde{\mathbf{s}}, \quad -\frac{1}{\sqrt{2N_t L}} \mathbf{1} \leq \tilde{\mathbf{s}} \leq \frac{1}{\sqrt{2N_t L}} \mathbf{1} \quad (25c)$$

Then, the scaled augmented Lagrangian function of (25) is written as

$$\begin{aligned} \mathcal{L}_{\rho_1, \rho_2}(\tilde{\mathbf{s}}, \mathbf{t}, \mathbf{r}, \mathbf{u}_1, \mathbf{u}_2) &= \frac{\mathbf{t}^T \tilde{\Phi}(\mathbf{w}) \mathbf{t}}{\mathbf{r}^T \tilde{\Gamma}(\mathbf{w}) \mathbf{r}} + \frac{\rho_1}{2} \|\mathbf{t} - \tilde{\mathbf{s}} + \mathbf{u}_1\|_2^2 \\ &\quad + \frac{\rho_2}{2} \|\mathbf{r} - \tilde{\mathbf{s}} + \mathbf{u}_2\|_2^2 \end{aligned} \quad (26)$$

where $\mathbf{u}_1, \mathbf{u}_2 \in \mathbb{R}^{2N_t L \times 1}$ are dual variables, and $\rho_1, \rho_2 > 0$ are penalty variables, which place penalties on the violations of primal feasibilities $\mathbf{t} = \tilde{\mathbf{s}}$ and $\mathbf{r} = \tilde{\mathbf{s}}$.

Under the ADMM framework, the following iterations need to be performed one by one:

$$\tilde{\mathbf{s}} \leftarrow \min_{\tilde{\mathbf{s}}} \mathcal{L}_{\rho_1, \rho_2}(\tilde{\mathbf{s}}, \mathbf{t}, \mathbf{r}, \mathbf{u}_1, \mathbf{u}_2), \text{ s.t. } \tilde{\mathbf{s}} \in \mathbb{D} \quad (27a)$$

$$\mathbf{t} \leftarrow \min_{\mathbf{t}} \mathcal{L}_{\rho_1, \rho_2}(\tilde{\mathbf{s}}, \mathbf{t}, \mathbf{r}, \mathbf{u}_1, \mathbf{u}_2), \text{ s.t. } \mathbf{t}^H \mathbf{t} = 1 \quad (27b)$$

$$\mathbf{r} \leftarrow \min_{\mathbf{r}} \mathcal{L}_{\rho_1, \rho_2}(\tilde{\mathbf{s}}, \mathbf{t}, \mathbf{r}, \mathbf{u}_1, \mathbf{u}_2) \quad (27c)$$

$$\mathbf{u}_1 \leftarrow \mathbf{u}_1 + (\mathbf{t} - \tilde{\mathbf{s}}), \quad \mathbf{u}_2 \leftarrow \mathbf{u}_2 + (\mathbf{r} - \tilde{\mathbf{s}}) \quad (27d)$$

where $\mathbb{D} = \{\tilde{\mathbf{s}} \mid -\frac{1}{\sqrt{2N_t L}} \mathbf{1} \leq \tilde{\mathbf{s}} \leq \frac{1}{\sqrt{2N_t L}} \mathbf{1}\}$.

In the sequel, the solutions to subproblems (27a)-(27c) are presented.

1) *Update of $\tilde{\mathbf{s}}$* : Omitting the constant term of the objective in subproblem (27a), the update of $\tilde{\mathbf{s}}$ needs to solve following problem:

$$\min_{\tilde{\mathbf{s}}} \frac{\rho_1 + \rho_2}{2} \tilde{\mathbf{s}}^T \tilde{\mathbf{s}} - \tilde{\mathbf{s}}^T \mathbf{b} \quad (28a)$$

$$\text{s.t. } -\frac{1}{\sqrt{2N_t L}} \mathbf{1} \leq \tilde{\mathbf{s}} \leq \frac{1}{\sqrt{2N_t L}} \mathbf{1} \quad (28b)$$

where $\mathbf{b} = \rho_1(\mathbf{t} + \mathbf{u}_1) + \rho_2(\mathbf{r} + \mathbf{u}_2)$. It is easy to notice that the problem (28) is a convex problem, and its closed-form solution can be obtained by the KKT condition [41], as

$$\tilde{s}_k = \begin{cases} \sqrt{\frac{1}{2N_t L}}, & \frac{b_k}{\rho_1 + \rho_2} \geq \sqrt{\frac{1}{2N_t L}} \\ \frac{b_k}{\rho_1 + \rho_2}, & -\sqrt{\frac{1}{2N_t L}} < \frac{b_k}{\rho_1 + \rho_2} < \sqrt{\frac{1}{2N_t L}} \\ -\sqrt{\frac{1}{2N_t L}}, & \frac{b_k}{\rho_1 + \rho_2} \leq -\sqrt{\frac{1}{2N_t L}} \end{cases} \quad (29)$$

where \tilde{s}_k and b_k are the k th entry of $\tilde{\mathbf{s}}$ and \mathbf{b} .

2) *Update of \mathbf{t}* : The subproblem w.r.t. \mathbf{t} is given by

$$\min_{\mathbf{t}} \frac{\mathbf{t}^T \tilde{\Phi}(\mathbf{w}) \mathbf{t}}{\mathbf{r}^T \tilde{\Gamma}(\mathbf{w}) \mathbf{r}} + \frac{\rho_1}{2} \|\mathbf{t} - \tilde{\mathbf{s}} + \mathbf{u}_1\|_2^2 \quad (30a)$$

$$\text{s.t. } \mathbf{t}^T \mathbf{t} = 1 \quad (30b)$$

The above problem is nonconvex due to the quadratic equality constraint. To solve it, let $\tilde{\Phi}(\mathbf{w}) = \mathbf{P} \mathbf{\Pi} \mathbf{P}^T$ denote the eigenvalue decomposition (EVD) of $\tilde{\Phi}(\mathbf{w})$, where $\mathbf{\Pi}$ is a diagonal matrix whose diagonal elements $\Pi_{k,k}$ ($k = 1, 2, \dots, 2N_t L$) are the eigenvalues of $\tilde{\Phi}(\mathbf{w})$, i.e., $\gamma_1 \geq \gamma_2 \geq \dots \geq \gamma_{2N_t L}$, and \mathbf{P} is a $2N_t L \times 2N_t L$ matrix whose columns are the corresponding right eigenvectors.

Then, using variable substitution, i.e., $\tilde{\mathbf{t}} = \mathbf{P}^T \mathbf{t}$ and $\mathbf{g} = \mathbf{P}^T(\tilde{\mathbf{s}} - \mathbf{u}_1)$, the optimization problem is reformulated as

$$\min_{\tilde{\mathbf{t}}} \eta \tilde{\mathbf{t}}^T \mathbf{\Pi} \tilde{\mathbf{t}} + \frac{\rho_1}{2} \|\tilde{\mathbf{t}} - \mathbf{g}\|_2^2 \quad (31a)$$

$$\text{s.t. } \tilde{\mathbf{t}}^T \tilde{\mathbf{t}} = 1 \quad (31b)$$

where $\eta = \frac{1}{\mathbf{r}^T \tilde{\Gamma}(\mathbf{w}) \mathbf{r}}$.

The Lagrange function of the problem (31) can be denoted as

$$\mathcal{L}(\tilde{\mathbf{t}}, \nu) = \eta \tilde{\mathbf{t}}^T \mathbf{\Pi} \tilde{\mathbf{t}} + \frac{\rho_1}{2} \|\tilde{\mathbf{t}} - \mathbf{g}\|_2^2 + \nu(\tilde{\mathbf{t}}^T \tilde{\mathbf{t}} - 1) \quad (32)$$

where ν is the Lagrange multiplier. Using the KKT condition [41], we obtain the first-order optimal condition of the problem (31), as

$$2\eta \mathbf{\Pi} \tilde{\mathbf{t}} + (\rho_1 + 2\nu) \tilde{\mathbf{t}} = \rho_1 \mathbf{g}, \quad \tilde{\mathbf{t}}^T \tilde{\mathbf{t}} = 1 \quad (33)$$

After some mathematical operations, we obtain that

$$\tilde{t}_k = \frac{\rho_1 g_k}{2\eta \gamma_k + \rho_1 + 2\nu}, \quad k = 1, 2, \dots, 2N_t L \quad (34)$$

and

$$f(\nu) = \sum_{k=1}^{2N_t L} \frac{\rho_1^2 g_k^2}{(2\eta \gamma_k + \rho_1 + 2\nu)^2} = 1 \quad (35)$$

where \tilde{t}_k and g_k are the k th element of $\tilde{\mathbf{t}}$ and \mathbf{g} , respectively.

Observing $f(\nu)$, since $\eta > 0$, $\rho_1 > 0$, and $\gamma_k > 0$ for all $k = 1, 2, \dots, 2N_t L$, $f(\nu)$ is monotonically increasing for $\nu \in (-\infty, -\eta\gamma_1 - 0.5\rho_1)$ and monotonically decreasing for $\nu \in (-\eta\gamma_{2N_t L} - 0.5\rho_1, \infty)$. Moreover, when $|\nu| \rightarrow \infty$, $f(\nu) \rightarrow 0$, and when $\nu \rightarrow -\eta\gamma_1 - 0.5\rho_1$ (or $-\eta\gamma_{2N_t L} - 0.5\rho_1$), $f(\nu)$ goes to infinity. Thus, $f(\nu) = 1$ has unique solution in $(-\infty, -\eta\gamma_1 - 0.5\rho_1)$ or $(-\eta\gamma_{2N_t L} - 0.5\rho_1, \infty)$, and the solution can be numerically solved by using the bisection method [41].

Finally, when ν is obtained, the optimal $\tilde{\mathbf{t}}$ can be computed by (34), and the solution to problem (30) is $\mathbf{t} = \mathbf{P} \tilde{\mathbf{t}}$.

3) *Update of r*: To update \mathbf{r} , we need to solve the following unconstrained problem:

$$\min_{\mathbf{r}} \frac{\mathbf{t}^T \tilde{\Phi}(\mathbf{w}) \mathbf{t}}{\mathbf{r}^T \tilde{\Gamma}(\mathbf{w}) \mathbf{r}} + \frac{\rho_2}{2} \|\mathbf{r} - \tilde{\mathbf{s}} + \mathbf{u}_2\|_2^2 \quad (36)$$

To attain its optimal solution, we let $\tilde{\Gamma}(\mathbf{w}) = \mathbf{U}\mathbf{\Lambda}\mathbf{U}^T$ be the EVD of $\tilde{\Gamma}$, where $\mathbf{\Lambda}$ is a diagonal matrix with the eigenvalues ($\lambda_1 \geq \lambda_2 \geq \dots \geq \lambda_{2N_t L}$).

Let $\tilde{\mathbf{r}} = \mathbf{U}^T \mathbf{r}$ and $\mathbf{q} = \mathbf{U}^T (\tilde{\mathbf{s}} - \mathbf{u}_2)$, the above problem is equivalent to

$$\min_{\tilde{\mathbf{r}}} \frac{\mathbf{t}^T \tilde{\Phi}(\mathbf{w}) \mathbf{t}}{\tilde{\mathbf{r}}^T \mathbf{\Lambda} \tilde{\mathbf{r}}} + \frac{\rho_2}{2} \|\tilde{\mathbf{r}} - \mathbf{q}\|_2^2 \quad (37)$$

Since the rank of $\Gamma(\mathbf{w})$ in (21) is 1, we can infer the rank of $\tilde{\Gamma}(\mathbf{w})$ is 2 from the definition of $\tilde{\Gamma}(\mathbf{w})$ in (22b), and the corresponding eigenvalues are equal, i.e.,

$$\lambda_1 = \lambda_2 > 0, \quad \lambda_k = 0, \quad k = 3, 4, \dots, 2N_t L \quad (38)$$

Thus, for $k = 3, 4, \dots, 2N_t L$, the optimal $\tilde{r}_k = q_k$, where \tilde{r}_k and q_k are the k th elements of $\tilde{\mathbf{r}}$ and \mathbf{q} .

To obtain optimal \tilde{r}_1 and \tilde{r}_2 , we need to solve following problem:

$$\min_{\tilde{r}_1, \tilde{r}_2} \frac{\mathbf{t}^T \tilde{\Phi}(\mathbf{w}) \mathbf{t}}{\lambda_1 \tilde{r}_1^2 + \lambda_2 \tilde{r}_2^2} + \frac{\rho_2}{2} [(\tilde{r}_1 - q_1)^2 + (\tilde{r}_2 - q_2)^2] \quad (39)$$

Let

$$\tilde{\lambda} = \lambda_1 = \lambda_2, p = 2 \frac{\mathbf{t}^T \tilde{\Phi}(\mathbf{w}) \mathbf{t}}{\tilde{\lambda} \rho_2} \quad (40)$$

A concise form of the above problem is given by

$$\min_{\tilde{r}_1, \tilde{r}_2} \frac{p}{\tilde{r}_1^2 + \tilde{r}_2^2} + (\tilde{r}_1 - q_1)^2 + (\tilde{r}_2 - q_2)^2 \quad (41)$$

To solve the problem (41), let function

$$\tilde{f}(\tilde{r}_1, \tilde{r}_2) = \frac{p}{\tilde{r}_1^2 + \tilde{r}_2^2} + (\tilde{r}_1 - q_1)^2 + (\tilde{r}_2 - q_2)^2 \quad (42)$$

Then, the optimal condition can be given by

$$\frac{\partial \tilde{f}(\tilde{r}_1, \tilde{r}_2)}{\partial \tilde{r}_1} = \frac{-2p\tilde{r}_1}{(\tilde{r}_1^2 + \tilde{r}_2^2)^2} + 2(\tilde{r}_1 - q_1) = 0 \quad (43a)$$

$$\frac{\partial \tilde{f}(\tilde{r}_1, \tilde{r}_2)}{\partial \tilde{r}_2} = \frac{-2p\tilde{r}_2}{(\tilde{r}_1^2 + \tilde{r}_2^2)^2} + 2(\tilde{r}_2 - q_2) = 0 \quad (43b)$$

After some mathematical operations, we obtain $q_2 \tilde{r}_1 = q_1 \tilde{r}_2$. Now, consider following discussions:

(a) If $q_1 = q_2 = 0$, according to (43), we have $\tilde{r}_1^2 + \tilde{r}_2^2 = \sqrt{p}$. Without prior information, the optimal solution that satisfies $\tilde{r}_1^2 + \tilde{r}_2^2 = \sqrt{p}$ can be randomly generated.

(b) If $q_1 \neq 0, q_2 = 0$, it is easy to know $\tilde{r}_2 = 0$. Substituting $\tilde{r}_2 = 0$ into (43) obtains $\tilde{r}_1^4 - q_1 \tilde{r}_1^3 - p = 0$ which is a quartic polynomial equation w.r.t. \tilde{r}_1 . Thus, the solution can be easily obtained by the formula of computing roots [42] or MATLAB software. Note that there may be more than one real root of the equation, and we need to select the one closest to q_1 .

(c) If $q_1 = 0, q_2 \neq 0$, this case is similar to case (b). We know $\tilde{r}_1 = 0$ and need to solve $\tilde{r}_2^4 - q_2 \tilde{r}_2^3 - p = 0$.

Algorithm 1 The ADMM method for solving problem (21).

Input: $\tilde{\mathbf{s}}^{(0)}, \mathbf{t}^{(0)}, \mathbf{r}^{(0)}, \mathbf{u}_1^{(0)}, \mathbf{u}_2^{(0)}$, penalty variables ρ_1 and ρ_2 , $\tilde{\Phi}(\mathbf{w})$ and $\tilde{\Gamma}(\mathbf{w})$, convergence tolerance $\epsilon > 0$, and some other system parameters that may be needed.

1: Set $n = 0$.

2: Perform EVD $\tilde{\Phi}(\mathbf{w}) = \mathbf{P}\mathbf{\Pi}\mathbf{P}^T$ and $\tilde{\Gamma}(\mathbf{w}) = \mathbf{U}\mathbf{\Lambda}\mathbf{U}^H$.

3: **repeat**

4: Set $n = n + 1$.

5: Update $\tilde{\mathbf{s}}^{(n)}$ by (29).

6: Solve $f(\nu) = 1$ via the bisection method.

7: Compute $\tilde{\mathbf{t}}^{(n)}$ by (34), then update $\mathbf{t}^{(n)} = \mathbf{P}\tilde{\mathbf{t}}^{(n)}$.

8: Let $\tilde{r}_k^{(n)} = q_k, k = 3, 4, \dots, 2N_t L$.

9: Compute $\tilde{r}_1^{(n)}, \tilde{r}_2^{(n)}$ by solving problem (41).

10: Update $\mathbf{r}^{(n)} = \mathbf{U}\tilde{\mathbf{r}}^{(n)}$.

11: Update $\mathbf{u}_1^{(n)} = \mathbf{u}_1^{(n-1)} + \mathbf{t}^{(n)} - \tilde{\mathbf{s}}^{(n)}$.

12: Update $\mathbf{u}_2^{(n)} = \mathbf{u}_2^{(n-1)} + \mathbf{r}^{(n)} - \tilde{\mathbf{s}}^{(n)}$.

13: **until** $\|\tilde{\mathbf{s}}^{(n)} - \mathbf{t}^{(n)}\|_2 \leq \epsilon$ and $\|\tilde{\mathbf{s}}^{(n)} - \mathbf{r}^{(n)}\|_2 \leq \epsilon$, or the maximal number of iterations is achieved.

Output: $\tilde{\mathbf{s}} = \tilde{\mathbf{s}}^{(n)}, \mathbf{t} = \mathbf{t}^{(n)}$, and $\mathbf{r} = \mathbf{r}^{(n)}$.

(d) If $q_1 \neq 0, q_2 \neq 0$, this is the most normal case. According to (43), the optimal \tilde{r}_1 can be obtained by solving

$$\tilde{r}_1^4 - q_1 \tilde{r}_1^3 - \frac{pq_1^4}{(q_1^2 + q_2^2)^2} = 0 \quad (44)$$

Then, the optimal \tilde{r}_2 is given by $\tilde{r}_2 = q_2 \tilde{r}_1 / q_1$. Finally, the \mathbf{r} is updated as $\mathbf{r} = \mathbf{U}\tilde{\mathbf{r}}$.

C. Complexity and Convergence Analysis

1) *Computational complexity*: The inner-loop is the implementation of the ADMM algorithm. The main computations include some matrix multiplications and the EVD of $\tilde{\Phi}(\mathbf{w})$ and $\tilde{\Gamma}(\mathbf{w})$. Since the EVD operations can be implemented in advance, the computational complexity of the inner-loop is about $\mathcal{O}(N_t^2 L^2)$. Note that, for the existing SDR and BCD methods, their computational complexities of the inner-loop are about $\mathcal{O}(N_t^{3.5} L^{3.5} + \mathcal{K} N_t^2 L^2)$ and $\mathcal{O}(N_t^3 L^3)$, respectively, where \mathcal{K} is the number of randomizations for the SDR method.

For the outer-loop, we need to perform the matrix inversion and EVD operations. Thus, the computational complexity per outer iteration is about $\mathcal{O}(N_r^3 L^3 + N_t^3 L^3 + I_{\text{ADMM}}^{\max} N_t^2 L^2)$, where I_{ADMM}^{\max} is the number of iteration in ADMM method.

2) *Convergence of the ADMM algorithm*: We use the following proposition to show the convergence of the ADMM algorithm.

Proposition 2: Defining residuals $\mathbf{d}^{(n+1)} = \tilde{\mathbf{s}}^{(n+1)} - \tilde{\mathbf{s}}^{(n)}$, $\mathbf{c}_1^{(n+1)} = \mathbf{t}^{(n+1)} - \tilde{\mathbf{s}}^{(n+1)}$, and $\mathbf{c}_2^{(n+1)} = \mathbf{r}^{(n+1)} - \tilde{\mathbf{s}}^{(n+1)}$, $\tilde{\mathbf{s}}^{(n+1)}$ converges to a KKT point of the problem (23) when $\mathbf{d}^{(n+1)} \rightarrow \mathbf{0}$, $\mathbf{c}_1^{(n+1)} \rightarrow \mathbf{0}$, and $\mathbf{c}_2^{(n+1)} \rightarrow \mathbf{0}$.

Proof: see **Appendix D**. ■

Note that in **Proposition 2**, the KKT conditions hold for problem (23) needs a strict condition, i.e., the residuals approach to zeros. Due to the fact that the formulated problem including the binary variables is a nonconvex problem, it is hard to prove that the residuals approach zeros as the iterations

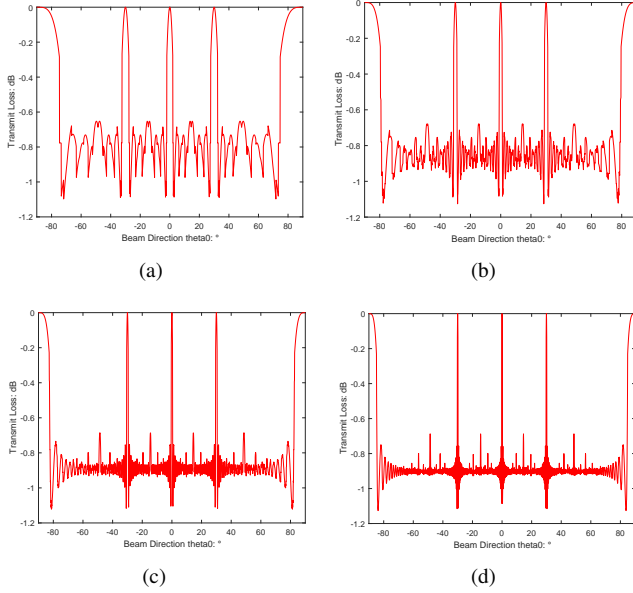


Fig. 2. Minimum transmit loss $L_t(\theta_0)$ for one-bit DACs versus different beam directions θ_0 . (a) $N_t = 8$; (b) $N_t = 16$; (c) $N_t = 32$; (d) $N_t = 64$.

going on. Nevertheless, this proposition is also useful, and in Sec. IV, we will verify the residuals of the proposed ADMM method are close to zeros via numerical simulation.

D. Performance Evaluation for One-bit MIMO Radar

In this subsection, the performance loss caused by using one-bit ADCs and DACs will be evaluated, respectively.

1) *Receive loss*: As mentioned earlier, compared with the MIMO radar with ideal ADCs, the loss of the QSINR with one-bit ADCs is about 1.96dB.

2) *Transmit loss*: To evaluate the transmit loss of using one-bit DACs, we consider the interference free case, i.e., $\Xi(\mathbf{s}) = \mathbf{0}$. Here, the output QSINR is simplified as

$$\text{QSINR}(\mathbf{w}, \mathbf{s}) = \frac{2 \text{SNR} |\mathbf{w}^H \mathbf{A}(\theta_0) \mathbf{s}|^2}{\pi \mathbf{w}^H \mathbf{w}} \quad (45)$$

and the optimal receive filter is the matched filter, i.e., $\mathbf{w}_M = \mathbf{A}(\theta_0) \mathbf{s} / \|\mathbf{A}(\theta_0) \mathbf{s}\|_2$. Plugging \mathbf{w}_M into $\text{QSINR}(\mathbf{w}, \mathbf{s})$, the transmit loss can be defined as

$$\begin{aligned} L_t(\theta_0) &= \mathbf{s}^H \mathbf{A}^H(\theta_0) \mathbf{A}(\theta_0) \mathbf{s} \\ &= \text{Tr}\{\mathbf{a}_r(\theta_0) \mathbf{a}_t^T(\theta_0) \mathbf{S} \mathbf{S}^H \mathbf{a}_t^*(\theta_0) \mathbf{a}_r^H(\theta_0)\} \\ &= \text{Tr}\{\mathbf{a}_t^T(\theta_0) \mathbf{S} \mathbf{S}^H \mathbf{a}_t^*(\theta_0)\} \\ &= \frac{1}{N_t^2 L} \sum_{l=1}^L \left| \sum_{k=1}^{N_t} e^{j\varphi_{k,l} - j\pi(k-1) \sin \theta_0} \right|^2 \end{aligned} \quad (46)$$

where $\text{Tr}(\cdot)$ is the trace operation and $\mathbf{S}(k, l) = \frac{1}{\sqrt{N_t L}} e^{j\varphi_{k,l}}$, $\varphi_{k,l} \in \{\frac{\pi}{4}, \frac{3\pi}{4}, \frac{5\pi}{4}, \frac{7\pi}{4}\}$.

Note that the larger $L_t(\theta_0)$ means the smaller QSINR loss. To maximize $L_t(\theta_0)$, the transmit signal needs to match the

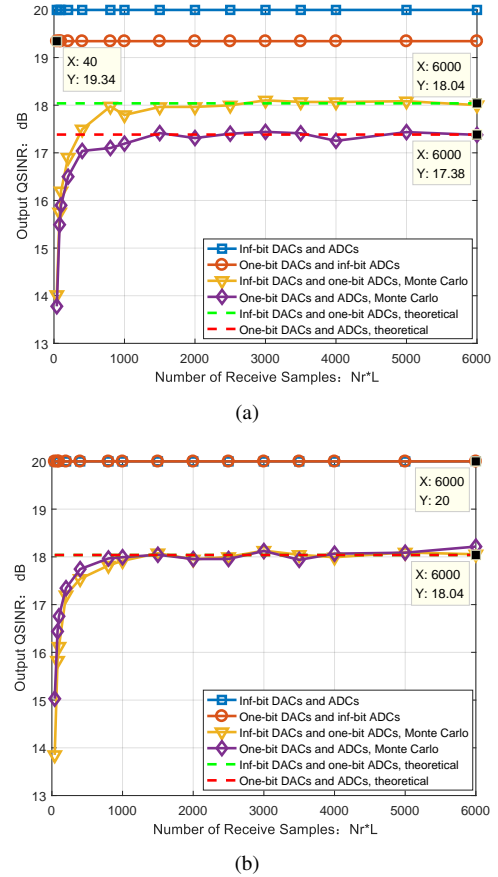


Fig. 3. The output QSINR (QSINR) of using different DACs/ADCs in noise-only case. (a) $\theta_0 = 15^\circ$; (b) $\theta_0 = 0^\circ$.

steering vector $\mathbf{a}_t(\theta_0)$ as much as possible. Thus, the $\varphi_{k,l}$ of the matched transmit signal \mathbf{S}_M should satisfy

$$\varphi_{k,l} = \begin{cases} \phi_l, & \text{mod}(\pi(k-1) \sin \theta_0, 2\pi) \in [0, \frac{1}{2}\pi) \\ \phi_l + \frac{1}{2}\pi, & \text{mod}(\pi(k-1) \sin \theta_0, 2\pi) \in [\frac{1}{2}\pi, \pi) \\ \phi_l + \pi, & \text{mod}(\pi(k-1) \sin \theta_0, 2\pi) \in [\pi, \frac{3}{2}\pi) \\ \phi_l + \frac{3}{2}\pi, & \text{mod}(\pi(k-1) \sin \theta_0, 2\pi) \in [\frac{3}{2}\pi, 2\pi) \end{cases} \quad (47)$$

where $\text{mod}(x, y)$ is the remainder after division of x by y , and ϕ_l is the reference phase which can be randomly selected from $\{\frac{\pi}{4}, \frac{3\pi}{4}, \frac{5\pi}{4}, \frac{7\pi}{4}\}$. Finally, substituting \mathbf{S}_M into $L_t(\theta_0)$ yields the minimum transmit loss for MIMO radar with one-bit DACs.

Note that, for different beam directions θ_0 , the transmit loss may be different. Fig. 2 gives the transmit loss versus different beam directions. As can be seen, the transmit losses at $\theta_0 = 0^\circ, \pm 30^\circ, \pm 90^\circ$ are 0dB. This is because that if $\sin \theta_0 = 0, \pm 0.5, \text{ or } \pm 1$, the steering vector $\mathbf{a}_t(\theta_0)$ can be perfectly matched by the one-bit transmit signal. For other beam directions, it is seen that the losses are about 0.9dB and no more than 1.2dB.

IV. SIMULATION RESULTS

In this section, several sets of simulations are provided to illustrate the performance of the proposed scheme. We first examine the performance of the proposed method under the noise-only case. Next, the case of interference existence with

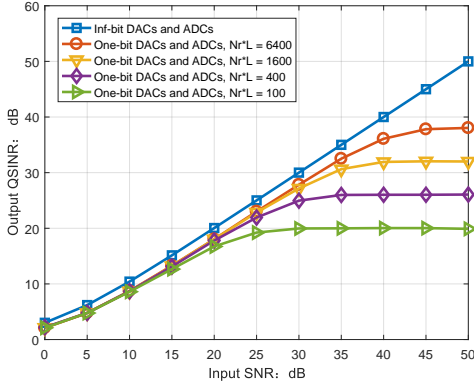


Fig. 4. The output QSINR (QSINR) versus different input SNR and number of receive samples, $\theta_0 = 0^\circ$.

known interference angles is considered. Finally, we assess the property of our method under the case where the angles of interferences are random variables.

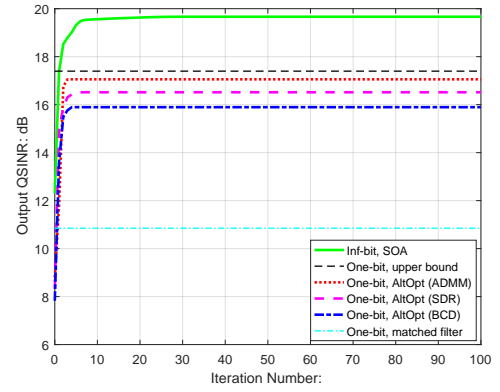
A. Noise-Only Case

In the first example, we consider the noise-only case, i.e., in the absence of interference. We set the number of transmit antennas $N_t = 8$, and we consider two beam directions $\theta_0 = 15^\circ$ and $\theta_0 = 0^\circ$, respectively. The noise power and input SNR are set to be $\sigma^2 = 1$ and $\text{SNR} = 20\text{dB}$. For the noise-only case, the optimal one-bit transmit signal can be obtained by (47), and the optimal receive filter is the matched filter, i.e., $\mathbf{w}_M = \mathbf{A}(\theta_0)\mathbf{s}/\|\mathbf{A}(\theta_0)\mathbf{s}\|_2$.

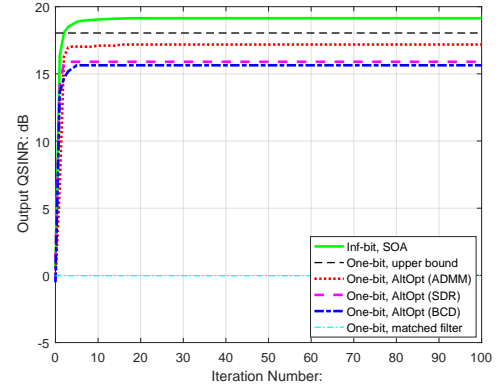
Fig. 3 plots the output QSINRs versus the number of receive samples $N_r L$ for MIMO radar with four different combinations of DACs/ADCs. Concretely, the four combinations are infinite-bit (denoted by “inf-bit”) DACs/ADCs, one-bit DACs and inf-bit ADCs, inf-bit DACs and one-bit ADCs, as well as one-bit DACs/ADCs. Additionally, for the last two combinations, we also perform 4000 Monte Carlo tests.

As shown in Fig. 3.(a), i.e., $\theta_0 = 15^\circ$, for MIMO radar with inf-bit DACs/ADCs, the maximal output QSINR is achieved, i.e., 20dB. While the losses of one-bit DACs and inf-bit ADCs, inf-bit DACs and one-bit ADCs, as well as one-bit DACs/ADCs are, 0.66dB, 1.96dB and 2.62 dB, respectively. From Fig. 3.(b), i.e., $\theta_0 = 0^\circ$, since $\theta_0 = 0^\circ$ is a special case in which the one-bit transmit signal is able to completely match the transmit steering vector, and thus the loss of using one-bit DACs is 0dB and the loss of one-bit ADCs and one-bit DACs is 1.96dB. Moreover, we also note that for a fixed SNR, as $N_r L$ increases, the gap between the theoretical QSINR and the one obtained by Monte Carlo tests becomes small. This is because the larger $N_r L$ results in a smaller input SNR of the single sample, i.e., $\text{SNR}_{\text{per}} = \text{SNR}/N_r L$, leading to the improved condition of **Lemma 1**. In fact, we find that when $N_r L \geq 1000$, i.e., $\text{SNR}_{\text{per}} \leq -10\text{dB}$, this gap is very small.

Next, we show the average QSINR as a function of the input SNR and number of receive samples in Fig. 4, where each point is obtained by performing 4000 independent Monte Carlo experiments. The angle of the target is assumed to be $\theta_0 = 0^\circ$. As expected, for traditional inf-bit MIMO radar, the



(a)



(b)

Fig. 5. The output QSINR in the presence of interferences, $N_t = 4$, $N_r = 8$, $L = 16$, three 30dB interferences $\theta_1 = -50^\circ$, $\theta_2 = -10^\circ$, and $\theta_3 = 40^\circ$. (a) $\theta_0 = 15^\circ$; (b) $\theta_0 = 0^\circ$.

output SINR is linear with the input SNR. However, for MIMO radar with one-bit ADCs/DACs, in low input SNR region, the change tendency of the QSINR is the same as that of the ideal output SINR, while in high input SNR region, the increasing tendency is slow. Moreover, the larger $N_r L$, the better the QSINR is able to achieve. This result is consistent with that in Fig. 3.

B. The Case of Interference Existence with Known Interference Angles

To facilitate comparison, in this example, we consider using the similar simulation parameters in [19], [20], where the numbers of transmit/receive antennas are $N_t = 4$ and $N_r = 8$, and the number of transmit waveform samples in one pulse is $L = 16$. Three interferences, with their INRs being 30dB and their directions being -50° , -10° , and 40° , are considered. The target angle is 15° or 0° , and the SNR is set to be 20dB. The inner ADMM algorithm sets $\mathbf{u}_1^{(0)} = \mathbf{u}_2^{(0)} = \mathbf{0}$ and the penalty variables $\rho_1 = 1$ and $\rho_2 = 7$, starts with random $\tilde{\mathbf{s}}^{(0)}$, $\mathbf{t}^{(0)}$, and $\mathbf{r}^{(0)}$, and terminates after 200 iterations.

Figs. 5 shows the curves of the output QSINR obtained by the different methods versus the number of iterations, where (a) is for $\theta_0 = 15^\circ$ and (b) is for $\theta_0 = 0^\circ$. For comparison purpose, the inf-bit joint design with the sequential optimization algorithm (SOA) [19], the one-bit joint designs

TABLE I
THE OPERATION TIME AND OUTPUT QSINR FOR ALTOPT FRAMEWORK USING THE SDR, BCD, AND ADMM METHODS (100 OUTER-LOOP ITERATIONS, PERFORMING ON A STANDARD PC WITH 16GB RAM AND 3.1 GHz CPU).

	L	16	32	64	128	256
time:s	SDR	47	390	3880	-	-
	BCD	0.35	1.16	6.51	53.4	790
	ADMM	2.63	3.72	7.66	38.2	231
QSINR:dB	SDR	16.54	16.30	16.32	-	-
	BCD	15.91	16.15	15.77	16.11	15.93
	ADMM	17.06	17.01	17.02	17.01	17.02

Note: “-” means that the method is not performed.

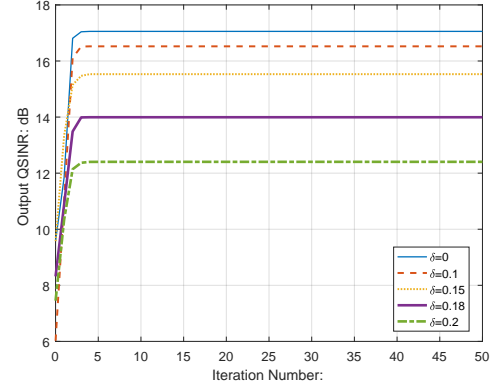
with the SDR [39] and BCD [40] are also considered. From Fig. 5, we note that for the cases of both $\theta_0 = 15^\circ$ and $\theta_0 = 0^\circ$, due to the presence of interference signals, the use of matched transmit signal and receive filter leads to a large QSINR loss. More importantly, it is observed that the proposed ADMM method outperforms the BCD and SDR methods in terms of the output QSINR. In addition, note that for one-bit MIMO radar, the QSINRs obtained by using the ADMM method are 17.06dB ($\theta_0 = 15^\circ$) and 17.18dB ($\theta_0 = 0^\circ$), which are very close to the theoretical upper bounds (obtained in noise-only case, i.e., 17.38dB ($\theta_0 = 15^\circ$) and 18.04dB ($\theta_0 = 0^\circ$)).

Table I analyzes the performance of the proposed ADMM, SDR and BCD with respect to the output QSINR values and computation time for $\theta_0 = 15^\circ$ and different number of samples $L = 16, 32, 64, 128, 256$. The results show that the proposed ADMM performs better than the other two methods in terms of the QSINR values. Furthermore, since the SDR has a high computational complexity of $\mathcal{O}(N_t^{3.5}L^{3.5})$ at each iteration, it takes the longest computation time, especially for large L . In addition, since the ADMM method has lower complexity, for large L , the ADMM method outperforms the BCD method in terms of the computational efficiency.

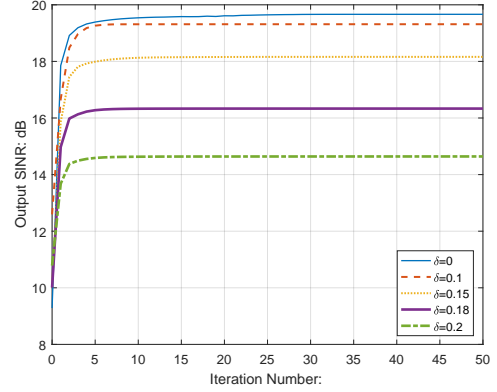
C. The Case of Interference Existence with unknown Interference Angles

In this example, we will evaluate the effect of the interference with angle uncertainties on the performance of the one-bit MIMO radar. Unless otherwise specified, the simulation parameters are same to the Sec. IV.B. Fig. 6 shows the output QSINR as a function of the number of iterations and the interference uncertainties. Here, the uncertainties of the three interferences are assumed to be same, i.e., $\delta_1 = \delta_2 = \delta_3 = \delta$. Note that $\delta = 0$ means that the interference angles are known. As expected, the output QSINR decreases as the uncertainty δ increases. Specifically, for one-bit MIMO radar, the corresponding output QSINRs in the figure are 17.06dB, 16.55dB, 15.55dB, 13.99dB, and 12.37dB, and for the traditional inf-bit MIMO radar, they are 19.66dB, 19.31dB, 18.16dB, 16.33dB, and 14.64dB.

Next, Fig. 7 plots the output QSINR versus the interference uncertainties with different INRs, i.e., $\text{INR}_k = \sigma_k^2/\sigma^2 =$



(a)



(b)

Fig. 6. The output QSINR for interferences with uncertainties, $\theta_0 = 15^\circ$. (a) One-bit MIMO radar; (b) inf-bit MIMO radar.

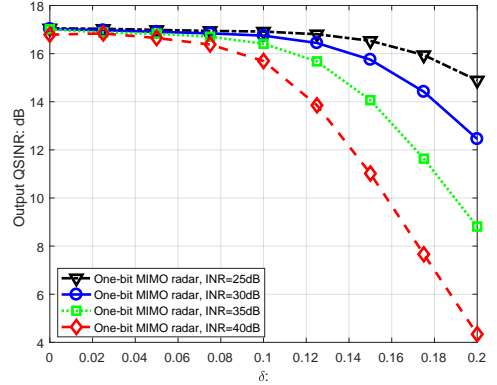


Fig. 7. The output QSINR for interferences with uncertainties and different INRs, $N_t = 4$, $N_r = 8$, and $\theta_0 = 15^\circ$.

25, 30, 35, 40dB ($k = 1, 2, 3$). It can be found that the output QSINR decreases with the INR increasing. In addition, for large interference uncertainties, the output QSINR is more sensitive to the INR. To enhance the interference suppression performance, we can increase the number of transmit and receive antennas. Specifically, we consider $N_t = 8$ and $N_r = 12$. The corresponding QSINR of the one-bit MIMO radar is shown in Fig. 8. It is seen that the interference suppression performance is significantly improved, especially for large δ .

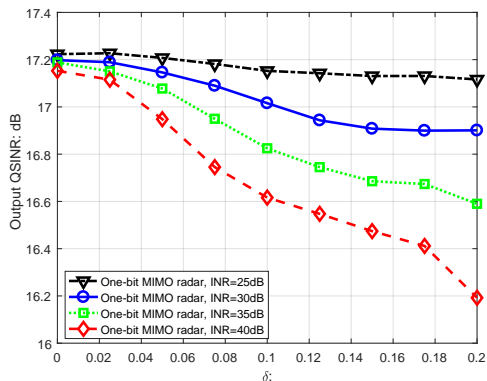
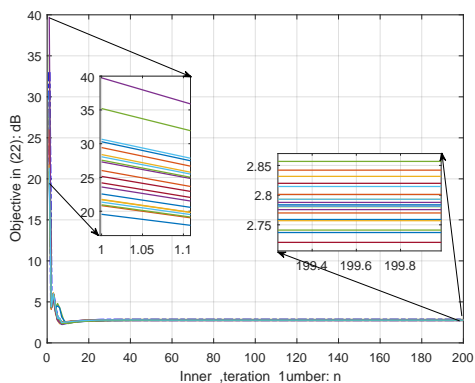
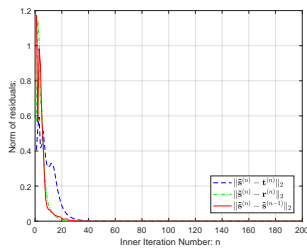


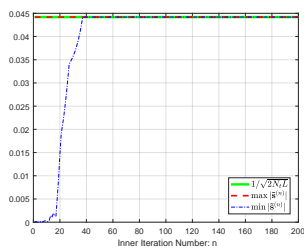
Fig. 8. The output QSINR of one-bit MIMO radar for interferences with uncertainties and different INRs, $N_t = 8$, $N_r = 12$, and $\theta_0 = 15^\circ$.



(a)



(b)



(c)

Fig. 9. Convergence property of the ADMM algorithm, $\rho_1 = 5$, $\rho_2 = 15$. (a) The objective value in problem (23) versus the iteration number with different initial points; (b) the norm of the residuals versus the iteration number; (c) the maximal and minimal modulus of $\bar{\mathbf{s}}$ versus the iteration number.

In the final example, the convergence property of the proposed method will be evaluated. Setting $N_t = 8$, $N_r = 12$, $L = 16$, $\delta = 0$, and $\text{INR}_k = 30\text{dB}$, firstly, we consider the convergence performance of the inner-loop iteration, i.e., the ADMM method. Specifically, we set $\rho_1 = 5$, $\rho_2 = 15$ and give a fixed \mathbf{w} . We perform the ADMM method for 20 times, for each test we set the initial point, including $\bar{\mathbf{s}}^{(0)}$, $\mathbf{t}^{(0)}$, and $\mathbf{r}^{(0)}$, as randomly variables, and terminate the method after 200 iterations. Fig. 9(a) shows the influence of the different initial points on the convergence of the ADMM method. The results show that the solutions with different initial points achieve similar values of the objective in problem (23), which indicates that the ADMM algorithm is not sensitive to the initial points.

Next, we also show the norms of the residuals (i.e., $\|\mathbf{d}^{(n)}\|_2$,

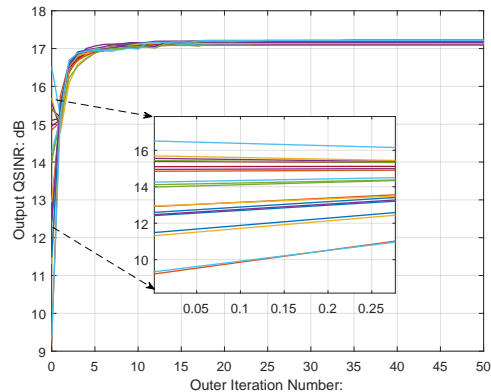


Fig. 10. The influence of different initial points on the outer-loop convergence.

$\|\mathbf{c}_1^{(n)}\|_2$, and $\|\mathbf{c}_2^{(n)}\|_2$) and the minimal and maximal modulus of $\bar{\mathbf{s}}^{(n)}$ versus the number of iterations in Fig. 9(b) and Fig. 9(c), respectively. It can be observed from Fig. 9(b) that with the iteration number increasing, the norms of the residuals tend to be zero. Based on the result in **Proposition 2**, since the norms of the residuals tend to be zero, we can infer that the obtained $\bar{\mathbf{s}}^{(n)}$ converges to the KKT point of problem (23). Moreover, the result in Fig. 9(c) displays the modulus of $\bar{\mathbf{s}}^{(n)}$ is close to a constant, i.e., $1/\sqrt{2N_tL}$, which means the waveform achieved by the proposed ADMM meets the constant modulus requirement.

Finally, we consider the convergence property of the outer-loop. Specifically, we randomly generate 20 initial points (i.e., \mathbf{s} to compute the \mathbf{w}) and perform the proposed alternating minimization algorithm with 50 iterations. Fig. 10 shows the output QSINR versus the number of outer-loop iterations with different initial points. The result shows that the solutions with different initial points achieve similar values of the output QSINR, indicating that the proposed algorithm is not sensitive to the initial points.

V. CONCLUSION

In this paper, we have proposed a novel MIMO radar with one-bit DACs and ADCs, named as one-bit MIMO radar. With the full or partial knowledge of the interferences, we have derived the output QSINR and formulated the problem of joint design of transmit waveform and receive filter for one-bit MIMO radar. An alternating optimization algorithm has been proposed to the resulting problem, in which the receive filter and transmit waveform were, respectively, obtained by solving a MVDR problem and using the ADMM framework. Moreover, in noise-only case, we have analyzed the empirical loss caused by using one-bit DACs, which is less than 1.2dB. In addition, compared with the traditional inf-bit ADCs, we have shown that when the number of receive samples is sufficiently large, the QSINR loss caused by using one-bit ADCs is about 1.96dB. The results have demonstrated that the MIMO radar can significantly reduce its system complexity via using one-bit DACs/ADCs at a cost of about 3dB QSINR loss.

APPENDIX A
PROOF OF PROPOSITION 1

Since $x_k \sim \mathcal{CN}(\tau_k, \sigma^2)$, $k = 1, 2$, and $\Re\{x_k\}$ and $\Im\{x_k\}$ are independent with each other, we have

$$\Re\{x_k\} \sim \mathcal{N}(\Re\{\tau_k\}, 0.5\sigma^2) \quad (48a)$$

$$\Im\{x_k\} \sim \mathcal{N}(\Im\{\tau_k\}, 0.5\sigma^2), \quad k = 1, 2 \quad (48b)$$

The probability of $\mathcal{Q}(\Re\{x_k\}) = 1$ can be denoted as

$$\begin{aligned} \mathcal{P}_{R,k} &= \mathcal{P}(\Re\{x_k\} > 0) \\ &= \frac{1}{\sqrt{\pi\sigma^2}} \int_0^\infty e^{-\frac{(t-\Re\{\tau_k\})^2}{\sigma^2}} dt \\ &= \frac{1}{2} + \frac{1}{2} \operatorname{erf}\left(\frac{\Re\{\tau_k\}}{\sigma}\right) \end{aligned} \quad (49)$$

Similarly, the probability of $\mathcal{Q}(\Im\{x_k\}) = 1$ is given by

$$\mathcal{P}_{I,k} = \frac{1}{2} + \frac{1}{2} \operatorname{erf}\left(\frac{\Im\{\tau_k\}}{\sigma}\right) \quad (50)$$

Moreover, the probabilities of $\mathcal{Q}(\Re\{x_k\}) = -1$ and $\mathcal{Q}(\Im\{x_k\}) = -1$ can be denoted as

$$\bar{\mathcal{P}}_{R,k} = 1 - \mathcal{P}_{R,k}, \quad \bar{\mathcal{P}}_{I,k} = 1 - \mathcal{P}_{I,k} \quad (51)$$

Consequently, we have

$$\mathcal{P}(y_k = 1 + j) = \mathcal{P}_{R,k} \mathcal{P}_{I,k} \quad (52a)$$

$$\mathcal{P}(y_k = 1 - j) = \mathcal{P}_{R,k} \bar{\mathcal{P}}_{I,k} \quad (52b)$$

$$\mathcal{P}(y_k = -1 + j) = \bar{\mathcal{P}}_{R,k} \mathcal{P}_{I,k} \quad (52c)$$

$$\mathcal{P}(y_k = -1 - j) = \bar{\mathcal{P}}_{R,k} \bar{\mathcal{P}}_{I,k}, \quad k = 1, 2 \quad (52d)$$

Then

$$\begin{aligned} \mathcal{P}(y_1 y_2^* = 2) &= \mathcal{P}_{R,1} \mathcal{P}_{I,1} \mathcal{P}_{R,2} \mathcal{P}_{I,2} + \mathcal{P}_{R,1} \bar{\mathcal{P}}_{I,1} \mathcal{P}_{R,2} \bar{\mathcal{P}}_{I,2} \\ &\quad + \bar{\mathcal{P}}_{R,1} \mathcal{P}_{I,1} \bar{\mathcal{P}}_{R,2} \mathcal{P}_{I,2} + \bar{\mathcal{P}}_{R,1} \bar{\mathcal{P}}_{I,1} \bar{\mathcal{P}}_{R,2} \bar{\mathcal{P}}_{I,2} \end{aligned} \quad (53a)$$

$$\begin{aligned} \mathcal{P}(y_1 y_2^* = -2) &= \mathcal{P}_{R,1} \mathcal{P}_{I,1} \bar{\mathcal{P}}_{R,2} \bar{\mathcal{P}}_{I,2} + \mathcal{P}_{R,1} \bar{\mathcal{P}}_{I,1} \bar{\mathcal{P}}_{R,2} \mathcal{P}_{I,2} \\ &\quad + \bar{\mathcal{P}}_{R,1} \mathcal{P}_{I,1} \mathcal{P}_{R,2} \bar{\mathcal{P}}_{I,2} + \bar{\mathcal{P}}_{R,1} \bar{\mathcal{P}}_{I,1} \mathcal{P}_{R,2} \mathcal{P}_{I,2} \end{aligned} \quad (53b)$$

$$\begin{aligned} \mathcal{P}(y_1 y_2^* = 2j) &= \mathcal{P}_{R,1} \mathcal{P}_{I,1} \mathcal{P}_{R,2} \bar{\mathcal{P}}_{I,2} + \mathcal{P}_{R,1} \bar{\mathcal{P}}_{I,1} \bar{\mathcal{P}}_{R,2} \bar{\mathcal{P}}_{I,2} \\ &\quad + \bar{\mathcal{P}}_{R,1} \mathcal{P}_{I,1} \mathcal{P}_{R,2} \mathcal{P}_{I,2} + \bar{\mathcal{P}}_{R,1} \bar{\mathcal{P}}_{I,1} \bar{\mathcal{P}}_{R,2} \mathcal{P}_{I,2} \end{aligned} \quad (53c)$$

$$\begin{aligned} \mathcal{P}(y_1 y_2^* = -2j) &= \mathcal{P}_{R,1} \mathcal{P}_{I,1} \bar{\mathcal{P}}_{R,2} \mathcal{P}_{I,2} + \mathcal{P}_{R,1} \bar{\mathcal{P}}_{I,1} \mathcal{P}_{R,2} \mathcal{P}_{I,2} \\ &\quad + \bar{\mathcal{P}}_{R,1} \mathcal{P}_{I,1} \bar{\mathcal{P}}_{R,2} \bar{\mathcal{P}}_{I,2} + \bar{\mathcal{P}}_{R,1} \bar{\mathcal{P}}_{I,1} \mathcal{P}_{R,2} \bar{\mathcal{P}}_{I,2} \end{aligned} \quad (53d)$$

Using (53), we obtain $\mathbb{E}\{\Re\{y_1 y_2^*\}\}$ and $\mathbb{E}\{\Im\{y_1 y_2^*\}\}$ in (54) and (55), respectively.

Finally, it is easy to verify that

$$\begin{aligned} \mathbb{E}\{y_1 y_2^*\} &= \mathbb{E}\{\Re\{y_1 y_2^*\}\} + j \mathbb{E}\{\Im\{y_1 y_2^*\}\} \\ &= \left[\operatorname{erf}\left(\frac{\Re\{\tau_1\}}{\sigma}\right) + j \operatorname{erf}\left(\frac{\Im\{\tau_1\}}{\sigma}\right) \right] \\ &\quad \times \left[\operatorname{erf}\left(\frac{\Re\{\tau_2\}}{\sigma}\right) - j \operatorname{erf}\left(\frac{\Im\{\tau_2\}}{\sigma}\right) \right] \end{aligned} \quad (56)$$

The proof is completed.

APPENDIX B
PROOF OF LEMMA 1

Let $f(x) = \operatorname{erf}(x)$, it is easy to see that $f(x)$ is continuous and differentiable w.r.t. x . We can obtain the first-order Taylor expansion of $f(x)$ at $x = 0$ as

$$\begin{aligned} f(x) &= f(0) + f'(0)(x - 0) + o(x) \\ &= \frac{2}{\sqrt{\pi}} x + o(x) \end{aligned} \quad (57)$$

where $f'(x) = \frac{2}{\sqrt{\pi}} e^{-x^2}$ is the first-order derivative and $o(x)$ is the high-order infinitesimal of x . Therefore, in the vicinity of $x = 0$, one gets $f(x) \approx \frac{2}{\sqrt{\pi}} x$.

When $|\tau_k| \ll \sigma$, $k = 1, 2$, we have $|\Re\{\tau_k\}| \ll \sigma$ and $|\Im\{\tau_k\}| \ll \sigma$. With this assumption, it can be noticed that

$$\frac{\Re\{\tau_k\}}{\sigma} \approx 0, \quad \frac{\Im\{\tau_k\}}{\sigma} \approx 0 \quad (58)$$

Therefore, we can obtain

$$\operatorname{erf}\left(\frac{\Re\{\tau_k\}}{\sigma}\right) = f\left(\frac{\Re\{\tau_k\}}{\sigma}\right) \approx \frac{2}{\sqrt{\pi}} \frac{\Re\{\tau_k\}}{\sigma} \quad (59a)$$

$$\operatorname{erf}\left(\frac{\Im\{\tau_k\}}{\sigma}\right) = f\left(\frac{\Im\{\tau_k\}}{\sigma}\right) \approx \frac{2}{\sqrt{\pi}} \frac{\Im\{\tau_k\}}{\sigma} \quad (59b)$$

Plugging (59) into (7) yields (8). Thus, the proof is completed.

APPENDIX C
COMPUTATIONS OF $\mathbf{C}(\omega_k)$ AND $\mathbf{D}(\omega_k)$

Consider the normalized angle $\omega = \sin \theta$ and let $\tilde{\mathbf{a}}_t(\omega) = \mathbf{a}_t(\theta)$ and $\tilde{\mathbf{a}}_r(\omega) = \mathbf{a}_r(\theta)$. Using some matrix operations, it is easy to have

$$\begin{aligned} \mathbf{A}(\theta) \mathbf{s} &= \operatorname{vec}\{\mathbf{a}_r(\theta) \mathbf{a}_t^T(\theta) \mathbf{S}\} = \operatorname{vec}\{\mathbf{a}_r(\omega) \mathbf{a}_t^T(\omega) \mathbf{S}\} \\ &= (\mathbf{S}^T \otimes \mathbf{I}_{N_r}) \operatorname{vec}\{\mathbf{a}_r(\omega) \mathbf{a}_t^T(\omega)\} \\ &= (\mathbf{S}^T \otimes \mathbf{I}_{N_r}) (\mathbf{a}_t(\omega) \otimes \mathbf{a}_r(\omega)) \end{aligned} \quad (60)$$

Then,

$$\mathbb{E}\{\mathbf{A}(\theta) \mathbf{s} \mathbf{s}^H \mathbf{A}^H(\theta)\} = (\mathbf{S}^T \otimes \mathbf{I}_{N_r}) \mathbf{C}(\omega) (\mathbf{S}^T \otimes \mathbf{I}_{N_r})^H \quad (61)$$

where

$$\begin{aligned} \mathbf{C}(\omega) &= \mathbb{E}\{(\mathbf{a}_t(\omega) \otimes \mathbf{a}_r(\omega)) (\mathbf{a}_t^H(\omega) \otimes \mathbf{a}_r^H(\omega))\} \\ &= \mathbb{E}\{\mathbf{a}_t(\omega) \mathbf{a}_t^H(\omega) \otimes \mathbf{a}_r(\omega) \mathbf{a}_r^H(\omega)\} \end{aligned} \quad (62)$$

Note that $\mathbf{C}(\omega) \in \mathbb{C}^{N_t N_r \times N_t N_r}$ is made up of $N_t \times N_t$ blocks, each of which is an $N_r \times N_r$ matrix.

Assume that ω obeys uniform distribution $\omega \sim \mathcal{U}(\varpi - \delta, \varpi + \delta)$. For the (m, n) th $(m, n = 1, 2, \dots, N_t)$ block of $\mathbf{C}(\omega)$, the (p, q) th $(p, q = 1, 2, \dots, N_r)$ element is given by

$$\begin{aligned} \mathbf{C}_{(m,n)}^{(p,q)}(\omega) &= \frac{1}{N_t N_r} \int_{\varpi - \delta}^{\varpi + \delta} \frac{1}{2\delta} e^{-j\pi(m-n+p-q)\omega} d\omega \\ &= \frac{e^{-j\pi(m-n+p-q)\varpi}}{N_t N_r} \operatorname{sinc}((m-n+p-q)\delta) \end{aligned} \quad (63)$$

where $\operatorname{sinc}(x) = \frac{\sin \pi x}{\pi x}$.

Considering $\omega = \omega_k$, $\omega_k \sim \mathcal{U}(\varpi_k - \delta_k, \varpi_k + \delta_k)$, $k = 1, 2, \dots, K$ and utilizing (63), we obtain $\mathbf{C}(\omega_k)$.

$$\begin{aligned}
\mathbb{E}\{\Re\{y_1 y_2^*\}\} &= 2\mathcal{P}(y_1 y_2^* = 2) - 2\mathcal{P}(y_1 y_2^* = -2) \\
&= 2\mathcal{P}_{R,1}\mathcal{P}_{I,1}(\mathcal{P}_{R,2}\mathcal{P}_{I,2} - \bar{\mathcal{P}}_{R,2}\bar{\mathcal{P}}_{I,2}) + 2\mathcal{P}_{R,1}\bar{\mathcal{P}}_{I,1}(\mathcal{P}_{R,2}\bar{\mathcal{P}}_{I,2} - \bar{\mathcal{P}}_{R,2}\mathcal{P}_{I,2}) \\
&\quad + 2\bar{\mathcal{P}}_{R,1}\mathcal{P}_{I,1}(\bar{\mathcal{P}}_{R,2}\mathcal{P}_{I,2} - \mathcal{P}_{R,2}\bar{\mathcal{P}}_{I,2}) + 2\bar{\mathcal{P}}_{R,1}\bar{\mathcal{P}}_{I,1}(\bar{\mathcal{P}}_{R,2}\bar{\mathcal{P}}_{I,2} - \mathcal{P}_{R,2}\mathcal{P}_{I,2}) \\
&= 2(\mathcal{P}_{R,1}\mathcal{P}_{I,1} - \bar{\mathcal{P}}_{R,1}\bar{\mathcal{P}}_{I,1})(\mathcal{P}_{R,2}\mathcal{P}_{I,2} - \bar{\mathcal{P}}_{R,2}\bar{\mathcal{P}}_{I,2}) + 2(\mathcal{P}_{R,1}\bar{\mathcal{P}}_{I,1} - \bar{\mathcal{P}}_{R,1}\mathcal{P}_{I,1})(\mathcal{P}_{R,2}\bar{\mathcal{P}}_{I,2} - \bar{\mathcal{P}}_{R,2}\mathcal{P}_{I,2}) \quad (54) \\
&= 4\mathcal{P}_{R,1}\mathcal{P}_{R,2} - 2\mathcal{P}_{R,1} - 2\mathcal{P}_{R,2} + 1 + 4\mathcal{P}_{I,1}\mathcal{P}_{I,2} - 2\mathcal{P}_{I,1} - 2\mathcal{P}_{I,2} + 1 \\
&= (2\mathcal{P}_{R,1} - 1)(2\mathcal{P}_{R,2} - 1) + (2\mathcal{P}_{I,1} - 1)(2\mathcal{P}_{I,2} - 1) \\
&= \operatorname{erf}\left(\frac{\Re\{\tau_1\}}{\sigma}\right) \operatorname{erf}\left(\frac{\Re\{\tau_2\}}{\sigma}\right) + \operatorname{erf}\left(\frac{\Im\{\tau_1\}}{\sigma}\right) \operatorname{erf}\left(\frac{\Im\{\tau_2\}}{\sigma}\right)
\end{aligned}$$

$$\begin{aligned}
\mathbb{E}\{\Im\{y_1 y_2^*\}\} &= 2\mathcal{P}(y_1 y_2^* = 2j) - 2\mathcal{P}(y_1 y_2^* = -2j) \\
&= 2\mathcal{P}_{R,1}\mathcal{P}_{I,1}(\mathcal{P}_{R,2}\bar{\mathcal{P}}_{I,2} - \bar{\mathcal{P}}_{R,2}\mathcal{P}_{I,2}) + 2\mathcal{P}_{R,1}\bar{\mathcal{P}}_{I,1}(\bar{\mathcal{P}}_{R,2}\bar{\mathcal{P}}_{I,2} - \mathcal{P}_{R,2}\mathcal{P}_{I,2}) \\
&\quad + 2\bar{\mathcal{P}}_{R,1}\mathcal{P}_{I,1}(\mathcal{P}_{R,2}\mathcal{P}_{I,2} - \bar{\mathcal{P}}_{R,2}\bar{\mathcal{P}}_{I,2}) + 2\bar{\mathcal{P}}_{R,1}\bar{\mathcal{P}}_{I,1}(\bar{\mathcal{P}}_{R,2}\mathcal{P}_{I,2} - \mathcal{P}_{R,2}\bar{\mathcal{P}}_{I,2}) \\
&= 2(\mathcal{P}_{R,1}\mathcal{P}_{I,1} - \bar{\mathcal{P}}_{R,1}\bar{\mathcal{P}}_{I,1})(\mathcal{P}_{R,2}\bar{\mathcal{P}}_{I,2} - \bar{\mathcal{P}}_{R,2}\mathcal{P}_{I,2}) + 2(\mathcal{P}_{R,1}\bar{\mathcal{P}}_{I,1} - \bar{\mathcal{P}}_{R,1}\mathcal{P}_{I,1})(\bar{\mathcal{P}}_{R,2}\bar{\mathcal{P}}_{I,2} - \mathcal{P}_{R,2}\mathcal{P}_{I,2}) \quad (55) \\
&= (4\mathcal{P}_{I,1}\mathcal{P}_{R,2} - 2\mathcal{P}_{I,1} - 2\mathcal{P}_{R,2} + 1) - (4\mathcal{P}_{R,1}\mathcal{P}_{I,2} - 2\mathcal{P}_{R,1} - 2\mathcal{P}_{I,2} + 1) \\
&= (2\mathcal{P}_{I,1} - 1)(2\mathcal{P}_{R,2} - 1) - (2\mathcal{P}_{R,1} - 1)(2\mathcal{P}_{I,2} - 1) \\
&= \operatorname{erf}\left(\frac{\Im\{\tau_1\}}{\sigma}\right) \operatorname{erf}\left(\frac{\Re\{\tau_2\}}{\sigma}\right) - \operatorname{erf}\left(\frac{\Re\{\tau_1\}}{\sigma}\right) \operatorname{erf}\left(\frac{\Im\{\tau_2\}}{\sigma}\right)
\end{aligned}$$

Similarly, to compute $\mathbf{D}(\omega_k)$, let us consider

APPENDIX D
PROOF OF PROPOSITION 2

$$\begin{aligned}
\mathbf{A}^H(\theta)\mathbf{w} &= \operatorname{vec}\{\mathbf{a}_t^*(\theta)\mathbf{a}_r^H(\theta)\mathbf{W}\} = \operatorname{vec}\{\mathbf{a}_t^*(\omega)\mathbf{a}_r^H(\omega)\mathbf{W}\} \\
&= (\mathbf{W}^T \otimes \mathbf{I}_{N_t})\operatorname{vec}\{\mathbf{a}_r^*(\omega)\mathbf{a}_t^H(\omega)\} \\
&= (\mathbf{W}^T \otimes \mathbf{I}_{N_t})(\mathbf{a}_r^*(\omega) \otimes \mathbf{a}_t^*(\omega)) \quad (64)
\end{aligned}$$

Then,

$$\mathbb{E}\{\mathbf{A}^H(\theta)\mathbf{w}\mathbf{w}^H\mathbf{A}(\theta)\} = (\mathbf{S}^T \otimes \mathbf{I}_{N_r})\mathbf{D}(\omega)(\mathbf{S}^T \otimes \mathbf{I}_{N_r})^H \quad (65)$$

where

$$\begin{aligned}
\mathbf{D}(\omega) &= \mathbb{E}\{(\mathbf{a}_r^*(\omega) \otimes \mathbf{a}_t^*(\omega))(\mathbf{a}_r^T(\omega) \otimes \mathbf{a}_t^T(\omega))\} \\
&= \mathbb{E}\{\mathbf{a}_r^*(\omega)\mathbf{a}_r^T(\omega) \otimes \mathbf{a}_t^*(\omega)\mathbf{a}_t^T(\omega)\} \quad (66)
\end{aligned}$$

is composed of $N_r \times N_r$ blocks, each of which is an $N_t \times N_t$ matrix.

For the (m, n) th $(m, n = 1, 2, \dots, N_r)$ block of $\mathbf{C}(\omega)$, the (p, q) th $(p, q = 1, 2, \dots, N_t)$ element is given by

$$\begin{aligned}
\mathbf{D}_{(m,n)}^{(p,q)}(\omega) &= \frac{1}{N_t N_r} \int_{-\varpi-\delta}^{\varpi+\delta} \frac{1}{2\delta} e^{j\pi(m-n+p-q)\omega} d\omega \\
&= \frac{e^{j\pi(m-n+p-q)\varpi}}{N_t N_r} \operatorname{sinc}((m-n+p-q)\delta) \quad (67)
\end{aligned}$$

Considering $\omega = \omega_k$, $\omega_k \sim \mathcal{U}(\varpi_k - \delta_k, \varpi_k + \delta_k)$ and utilizing (67), we obtain $\mathbf{D}(\omega_k)$.

The KKT condition of the problem (23) can be given by

$$\frac{2\tilde{\Phi}(\mathbf{w})\tilde{\mathbf{s}}}{\tilde{\mathbf{s}}^T \tilde{\Gamma}(\mathbf{w})\tilde{\mathbf{s}}} - \frac{2\tilde{\mathbf{s}}^T \tilde{\Phi}(\mathbf{w})\tilde{\mathbf{s}} \tilde{\Gamma}(\mathbf{w})\tilde{\mathbf{s}}}{(\tilde{\mathbf{s}}^T \tilde{\Gamma}(\mathbf{w})\tilde{\mathbf{s}})^2} + \vartheta_u - \vartheta_l + 2\nu\tilde{\mathbf{s}} = \mathbf{0} \quad (68a)$$

$$\tilde{\mathbf{s}}^T \tilde{\mathbf{s}} = 1, \quad \frac{-1}{\sqrt{2N_t L}} \mathbf{1} \leq \tilde{\mathbf{s}} \leq \frac{1}{\sqrt{2N_t L}} \mathbf{1} \quad (68b)$$

$$\vartheta_u \odot (\tilde{\mathbf{s}} - \frac{1}{\sqrt{2N_t L}} \mathbf{1}) = \mathbf{0}, \quad \vartheta_u \geq \mathbf{0} \quad (68c)$$

$$\vartheta_l \odot (\tilde{\mathbf{s}} + \frac{1}{\sqrt{2N_t L}} \mathbf{1}) = \mathbf{0}, \quad \vartheta_l \geq \mathbf{0} \quad (68d)$$

where ν , ϑ_u , and ϑ_l are dual variables.

According to the update rule in (27), firstly, $\tilde{\mathbf{s}}^{(n+1)}$ is obtained by minimizing $\frac{\rho_1}{2} \|\mathbf{t}^{(n)} - \tilde{\mathbf{s}} + \mathbf{u}_1^{(n)}\|_2^2 + \frac{\rho_2}{2} \|\mathbf{r}^{(n)} - \tilde{\mathbf{s}} + \mathbf{u}_2^{(n)}\|_2^2$ subject to $\tilde{\mathbf{s}} \in \mathbb{D}$, and thus $\tilde{\mathbf{s}}^{(n+1)}$ satisfies

$$\begin{aligned}
\rho_1(\tilde{\mathbf{s}}^{(n+1)} - \mathbf{t}^{(n)} - \mathbf{u}_1^{(n)}) + \rho_2(\tilde{\mathbf{s}}^{(n+1)} - \mathbf{r}^{(n)} - \mathbf{u}_2^{(n)}) \\
+ \vartheta_u^{(n+1)} - \vartheta_l^{(n+1)} = \mathbf{0} \quad (69)
\end{aligned}$$

where $\vartheta_u^{(n+1)}$ and $\vartheta_l^{(n+1)}$ satisfy (68c) and (68d).

Secondly, subject to $\mathbf{t}^T \mathbf{t} = 1$, $\mathbf{t}^{(n+1)}$ is updated by solving $\min_{\mathbf{t}} \mathcal{L}_{\rho_1, \rho_2}(\tilde{\mathbf{s}}^{(n+1)}, \mathbf{t}, \mathbf{r}^{(n)}, \mathbf{u}_1^{(n)}, \mathbf{u}_2^{(n)})$. Therefore, we have

$$\begin{aligned}
\frac{2\tilde{\Phi}(\mathbf{w})\mathbf{t}^{(n+1)}}{(\mathbf{r}^{(n)})^T \tilde{\Gamma}(\mathbf{w})\mathbf{r}^{(n)}} + \rho_1(\mathbf{t}^{(n+1)} - \tilde{\mathbf{s}}^{(n+1)} + \mathbf{u}_1^{(n)}) \\
+ 2\nu^{(n+1)} \mathbf{t}^{(n+1)} = \mathbf{0} \quad (70)
\end{aligned}$$

In addition, $\mathbf{r}^{(n+1)}$ is obtained by solving the unconstrained problem $\min_{\mathbf{r}} \mathcal{L}_{\rho_1, \rho_2}(\tilde{\mathbf{s}}^{(n+1)}, \mathbf{t}^{(n+1)}, \mathbf{r}, \mathbf{u}_1^{(n)}, \mathbf{u}_2^{(n)})$,

which yields

$$\begin{aligned} & - \frac{2(\mathbf{t}^{(n+1)})^T \tilde{\Phi}(\mathbf{w}) \mathbf{t}^{(n+1)} \tilde{\Gamma}(\mathbf{w}) \mathbf{r}^{(n+1)}}{((\mathbf{r}^{(n+1)})^T \tilde{\Gamma}(\mathbf{w}) \mathbf{r}^{(n+1)})^2} \\ & + \rho_2 (\mathbf{r}^{(n+1)} - \tilde{\mathbf{s}}^{(n+1)} + \mathbf{u}_2^{(n)}) = \mathbf{0} \end{aligned} \quad (71)$$

Finally, combining the above three equations (69)-(71) and using $\mathbf{d}^{(n+1)}, \mathbf{c}_1^{(n+1)}, \mathbf{c}_2^{(n+1)} \rightarrow \mathbf{0}$, we have

$$\begin{aligned} & \frac{2\tilde{\Phi}(\mathbf{w})\tilde{\mathbf{s}}^{(n+1)}}{(\tilde{\mathbf{s}}^{(n+1)})^T \tilde{\Gamma}(\mathbf{w}) \tilde{\mathbf{s}}^{(n+1)}} - \frac{2(\tilde{\mathbf{s}}^{(n+1)})^T \tilde{\Phi}(\mathbf{w}) \tilde{\mathbf{s}}^{(n+1)} \tilde{\Gamma}(\mathbf{w}) \tilde{\mathbf{s}}^{(n+1)}}{((\tilde{\mathbf{s}}^{(n+1)})^T \tilde{\Gamma}(\mathbf{w}) \tilde{\mathbf{s}}^{(n+1)})^2} \\ & + \vartheta_u^{(n+1)} - \vartheta_l^{(n+1)} + 2\nu^{(n+1)} \tilde{\mathbf{s}}^{(n+1)} = \mathbf{0} \end{aligned} \quad (72)$$

As a result, $\tilde{\mathbf{s}}^{(n+1)}$ satisfies the KKT condition (68), and the proof is completed.

REFERENCES

- [1] J. Li and P. Stoica, "MIMO Radar with Colocated Antennas," *IEEE Signal Process. Mag.*, vol. 24, no. 5, pp. 106–114, Sep. 2007.
- [2] Jian Li, P. Stoica, Luzhou Xu, and W. Roberts, "On Parameter Identifiability of MIMO Radar," *IEEE Signal Process. Lett.*, vol. 14, no. 12, pp. 968–971, Dec. 2007.
- [3] X. Zhang, L. Xu, L. Xu, and D. Xu, "Direction of Departure (DOD) and Direction of Arrival (DOA) Estimation in MIMO Radar with Reduced-Dimension MUSIC," *IEEE Commun. Lett.*, vol. 14, no. 12, pp. 1161–1163, Dec. 2010.
- [4] A. Khabbazi-basmenj, A. Hassanien, S. A. Vorobyov, and M. W. Morency, "Efficient Transmit BeamSpace Design for Search-Free Based DOA Estimation in MIMO Radar," *IEEE Trans. Signal Process.*, vol. 62, no. 6, pp. 1490–1500, Mar. 2014.
- [5] P. Stoica, Jian Li, and Yao Xie, "On Probing Signal Design For MIMO Radar," *IEEE Trans. Signal Process.*, vol. 55, no. 8, pp. 4151–4161, Aug. 2007.
- [6] D. Fuhrmann and G. San Antonio, "Transmit beamforming for MIMO radar systems using signal cross-correlation," *IEEE Trans. Aerosp. Electron. Syst.*, vol. 44, no. 1, pp. 171–186, Jan. 2008.
- [7] S. Ahmed, J. S. Thompson, Y. R. Petillot, and B. Mulgrew, "Unconstrained Synthesis of Covariance Matrix for MIMO Radar Transmit Beampattern," *IEEE Trans. Signal Process.*, vol. 59, no. 8, pp. 3837–3849, Aug. 2011.
- [8] A. Aubry, M. Lops, A. M. Tulino, and L. Venturino, "On MIMO Detection Under Non-Gaussian Target Scattering," *IEEE Trans. Inform. Theory*, vol. 56, no. 11, pp. 5822–5838, Nov. 2010.
- [9] B. Friedlander, "Waveform Design for MIMO Radars," *IEEE Trans. Aerosp. Electron. Syst.*, vol. 43, no. 3, pp. 1227–1238, Jul. 2007.
- [10] Jian Li, Luzhou Xu, P. Stoica, K. Forsythe, and D. Bliss, "Range Compression and Waveform Optimization for MIMO Radar: A Cramér-Rao Bound Based Study," *IEEE Trans. Signal Process.*, vol. 56, no. 1, pp. 218–232, Jan. 2008.
- [11] Z. Cheng, B. Liao, S. Shi, Z. He, and J. Li, "Co-Design for Overlaid MIMO Radar and Downlink MISO Communication Systems via Cramér-Rao Bound Minimization," *IEEE Trans. Signal Process.*, vol. 67, no. 24, pp. 6227–6240, Dec. 2019.
- [12] Y. Yang and R. Blum, "MIMO radar waveform design based on mutual information and minimum mean-square error estimation," *IEEE Trans. Aerosp. Electron. Syst.*, vol. 43, no. 1, pp. 330–343, Jan. 2007.
- [13] A. De Maio and M. Lops, "Design Principles of MIMO Radar Detectors," *IEEE Trans. Aerosp. Electron. Syst.*, vol. 43, no. 3, pp. 886–898, Jul. 2007.
- [14] B. Tang and J. Li, "Spectrally Constrained MIMO Radar Waveform Design Based on Mutual Information," *IEEE Trans. Signal Process.*, vol. 67, no. 3, pp. 821–834, Feb. 2019.
- [15] T. Bouchoucha, S. Ahmed, T. Al-Naffouri, and M.-S. Alouini, "DFT-Based Closed-Form Covariance Matrix and Direct Waveforms Design for MIMO Radar to Achieve Desired Beampatterns," *IEEE Trans. Signal Process.*, vol. 65, no. 8, pp. 2104–2113, Apr. 2017.
- [16] K. Alhujaili, V. Monga, and M. Rangaswamy, "Transmit MIMO Radar Beampattern Design via Optimization on the Complex Circle Manifold," *IEEE Trans. Signal Process.*, vol. 67, no. 13, pp. 3561–3575, Jul. 2019.
- [17] Z. Cheng, Z. He, S. Zhang, and J. Li, "Constant Modulus Waveform Design for MIMO Radar Transmit Beampattern," *IEEE Trans. Signal Process.*, vol. 65, no. 18, pp. 4912–4923, Sep. 2017.
- [18] C.-Y. Chen and P. P. Vaidyanathan, "MIMO Radar Space-Time Adaptive Processing Using Prolate Spheroidal Wave Functions," *IEEE Trans. Signal Process.*, vol. 56, no. 2, pp. 623–635, Feb. 2008.
- [19] G. Cui, H. Li, and M. Rangaswamy, "MIMO Radar Waveform Design With Constant Modulus and Similarity Constraints," *IEEE Trans. Signal Process.*, vol. 62, no. 2, pp. 343–353, Jan. 2014.
- [20] Z. Cheng, Z. He, B. Liao, and M. Fang, "MIMO Radar Waveform Design With PAPR and Similarity Constraints," *IEEE Trans. Signal Process.*, vol. 66, no. 4, pp. 968–981, Feb. 2018.
- [21] S. Boyd, "Distributed Optimization and Statistical Learning via the Alternating Direction Method of Multipliers," *Foundations and Trends® in Machine Learning*, vol. 3, no. 1, pp. 1–122, 2010.
- [22] Y. Yu, A. P. Petropulu, and H. V. Poor, "MIMO Radar Using Compressive Sampling," *IEEE J. Sel. Top. Signal Process.*, vol. 4, no. 1, pp. 146–163, Feb. 2010.
- [23] M. Rossi, A. M. Haimovich, and Y. C. Eldar, "Spatial Compressive Sensing for MIMO Radar," *IEEE Trans. Signal Process.*, vol. 62, no. 2, pp. 419–430, Jan. 2014.
- [24] D. Cohen, D. Cohen, Y. C. Eldar, and A. M. Haimovich, "SUMMeR: Sub-Nyquist MIMO Radar," *IEEE Trans. Signal Process.*, vol. 66, no. 16, pp. 4315–4330, Aug. 2018.
- [25] K. V. Mishra, Y. C. Eldar, E. Shoshan, M. Namer, and M. Meltsin, "A Cognitive Sub-Nyquist MIMO Radar Prototype," *IEEE Trans. Aerosp. Electron. Syst.*, vol. 56, no. 2, pp. 937–955, Apr. 2020.
- [26] E. Candes and M. Wakin, "An Introduction To Compressive Sampling," *IEEE Signal Process. Mag.*, vol. 25, no. 2, pp. 21–30, Mar. 2008.
- [27] C. Kong, A. Mezghani, C. Zhong, A. L. Swindlehurst, and Z. Zhang, "Nonlinear Precoding for Multipair Relay Networks With One-Bit ADCs and DACs," *IEEE Signal Process. Lett.*, vol. 25, no. 2, pp. 303–307, Feb. 2018.
- [28] F. Sohrabi, Y.-F. Liu, and W. Yu, "One-Bit Precoding and Constellation Range Design for Massive MIMO With QAM Signaling," *IEEE J. Sel. Top. Signal Process.*, vol. 12, no. 3, pp. 557–570, Jun. 2018.
- [29] A. Mezghani and A. L. Swindlehurst, "Blind Estimation of Sparse Broadband Massive MIMO Channels With Ideal and One-bit ADCs," *IEEE Trans. Signal Process.*, vol. 66, no. 11, pp. 2972–2983, Jun. 2018.
- [30] Y.-S. Jeon, N. Lee, S.-N. Hong, and R. W. Heath, "One-Bit Sphere Decoding for Uplink Massive MIMO Systems With One-Bit ADCs," *IEEE Trans. Wireless Commun.*, vol. 17, no. 7, pp. 4509–4521, Jul. 2018.
- [31] A. Ameri, A. Bose, J. Li, and M. Soltanalian, "One-Bit Radar Processing With Time-Varying Sampling Thresholds," *IEEE Trans. Signal Process.*, vol. 67, no. 20, pp. 5297–5308, Oct. 2019.
- [32] B. Zhao, L. Huang, and W. Bao, "One-Bit SAR Imaging Based on Single-Frequency Thresholds," *IEEE Trans. Geosci. Remote Sensing*, vol. 57, no. 9, pp. 7017–7032, Sep. 2019.
- [33] B. Jin, J. Zhu, Q. Wu, Y. Zhang, and Z. Xu, "One-Bit LFMCW Radar: Spectrum Analysis and Target Detection," *IEEE Trans. Aerosp. Electron. Syst.*, vol. 56, no. 4, pp. 2732–2750, Aug. 2020.
- [34] Z. Cheng, Z. He, and B. Liao, "Target Detection Performance of Collocated MIMO Radar With One-Bit ADCs," *IEEE Signal Process. Lett.*, vol. 26, no. 12, pp. 1832–1836, Dec. 2019.
- [35] F. Xi, Y. Xiang, Z. Zhang, S. Chen, and A. Nehorai, "Joint Angle and Doppler Frequency Estimation for MIMO Radar with One-Bit Sampling: A Maximum Likelihood-Based Method," *IEEE Trans. Aerosp. Electron. Syst.*, vol. 56, no. 6, pp. 4734–4748, Dec. 2020.
- [36] F. Xi, Y. Xiang, S. Chen, and A. Nehorai, "Gridless Parameter Estimation for One-Bit MIMO Radar With Time-Varying Thresholds," *IEEE Trans. Signal Process.*, vol. 68, pp. 1048–1063, 2020.
- [37] Z. Cheng, B. Liao, Z. He, and J. Li, "Transmit Signal Design for Large-Scale MIMO System With 1-bit DACs," *IEEE Trans. Wireless Commun.*, vol. 18, no. 9, pp. 4466–4478, Sep. 2019.
- [38] Z. Cheng, S. Shi, Z. He, and B. Liao, "Transmit Sequence Design for Dual-Function Radar-Communication System With One-Bit DACs," *IEEE Trans. Wireless Commun.*, pp. 1–1, 2021.
- [39] Z.-q. Luo, W.-k. Ma, A. So, Y. Ye, and S. Zhang, "Semidefinite Relaxation of Quadratic Optimization Problems," *IEEE Signal Process. Mag.*, vol. 27, no. 3, pp. 20–34, May 2010.
- [40] M. Hong, M. Razaviyayn, Z. Q. Luo, and J. S. Pang, "A unified algorithmic framework for block-structured optimization involving big data: With applications in machine learning and signal processing," *IEEE Signal Process. Mag.*, vol. 33, no. 1, pp. 57–77, Jan. 2016.
- [41] S. Boyd and L. Vandenberghe, *Convex Optimization*. UK: Cambridge Univ. Press, 2004.
- [42] Wikipedia. Quartic equation. [Online]. Available: https://en.wikipedia.org/wiki/Quartic_equation